

# Epsilon-negative media from the viewpoint of materials science

Guohua Fan<sup>1</sup>, Kai Sun<sup>2</sup>, Qing Hou<sup>3</sup>, Zhongyang Wang<sup>4</sup>, Yao Liu<sup>1,\*</sup>, and Runhua Fan<sup>1,2,\*\*</sup>

<sup>1</sup> Key Laboratory for Liquid-Solid Structural Evolution and Processing of Materials (Ministry of Education), Shandong University, Jinan 250061, PR China

<sup>2</sup> College of Ocean Science and Engineering, Shanghai Maritime University, Shanghai 201306, PR China

<sup>3</sup> Department of Chemistry, University College London, London WC1H 0AJ, UK

<sup>4</sup> State Key Lab of Metal Matrix Composites, School of Materials Science and Engineering, Shanghai Jiao Tong University, Shanghai 200240, PR China

Received: 11 November 2020 / Accepted: 14 March 2021

**Abstract.** A comprehensive review of the fundamentals and applications of epsilon-negative materials is presented in this paper. Percolative composites, as well as homogeneous ceramics or polymers, have been investigated to obtain the tailorable epsilon-negative properties. It's confirmed the anomalous epsilon-negative property can be realized in conventional materials. Meanwhile, from the perspective of materials science, the relationship between the negative permittivity and the composition and microstructure of materials has been clarified. It's demonstrated that the epsilon-negative performance is attributed to the plasmonic response of delocalized electrons within the materials and can be modulated by it. Moreover, the potential applications of epsilon-negative materials in electromagnetic interference shielding, laminated composites for multilayered capacitance, coil-less electric inductors, and epsilon-near-zero metamaterials are reviewed. The development of epsilon-negative materials has enriched the connotation of metamaterials and advanced functional materials, and has accelerated the integration of metamaterials and natural materials.

**Keywords:** Epsilon-negative materials / negative permittivity / percolative composites / electromagnetic shielding / laminated dielectrics

## 1 Introduction

Permittivity and permeability are two basic physical parameters of materials, which characterize the response of materials in electric, magnetic, or electromagnetic fields [1–3]. According to the sign of permittivity and permeability, materials are classified into four quadrants, including common materials, double-negative materials, mu-negative materials, and epsilon-negative materials, as shown in Figure 1 [4,5]. Common materials with positive permittivity and positive permeability are transparent to the incident electromagnetic waves, and electric vector ( $E$ ), magnetic vector ( $B$ ), and the wave vector ( $k$ ) correspond to right-handed rule. For materials with double negative parameters, like metamaterials, electromagnetic waves can also propagate within them but the relationships among  $E$ ,  $B$ , and  $k$  are left-handed. Electromagnetic waves decay evanescently in materials with only negative permittivity or negative permeability. Mu-negative materials could be

realized with some ferrites at their magnetic resonance frequency, while the modulation of epsilon-negative properties was firstly realized in metamaterials [6]. Metamaterials are a kind of artificial materials composed of periodic building blocks with a series of novel physical properties which are rarely seen in natural materials [7,8]. The construction techniques of metamaterials provide approaches to obtain new kinds of electromagnetic medium with anomalous negative physical parameters. Arrays of the periodic metallic units are essential to achieve negative electromagnetic parameters [9]. The realization and regulation of the performance of metamaterials are dependent on the excitation of the geometries and configurations of the building blocks, which is almost independent on the composition of the components. It can also be considered that the unique properties of metamaterials are artificially designed electromagnetic properties, rather than being determined by the composition and microstructure of the materials.

From the perspective of materials science, the physical properties of a material must depend on its composition and microstructure, which explains the structure-activity

\* e-mail: [liuyao@sdu.edu.cn](mailto:liuyao@sdu.edu.cn)

\*\* e-mail: [rhfan@shmtu.edu.cn](mailto:rhfan@shmtu.edu.cn)

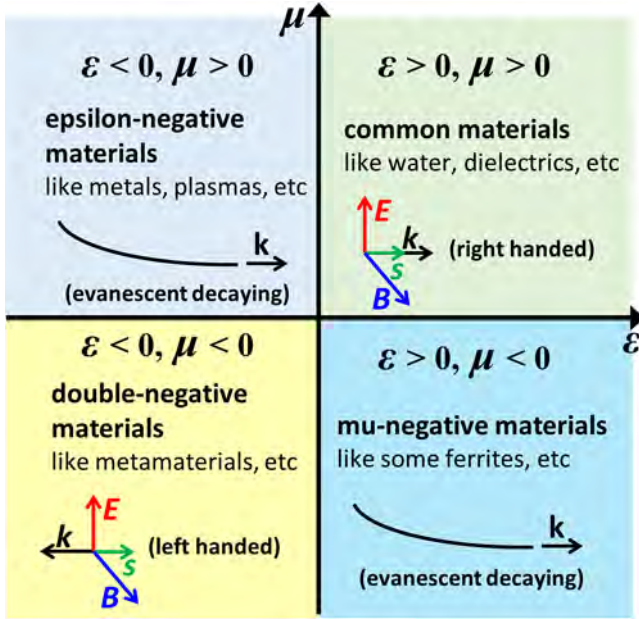


**Fig. 1.** Categories of materials according to their permittivity ( $\epsilon$ ) and permeability ( $\mu$ ) [4,5].

relationships of materials and enlightens researchers to improve the properties of the materials through altering composition and tailoring microstructure of the constitutive components within materials [10,11]. So, can the “real” materials realize the properties of metamaterials, such as the negative permittivity and/or the negative permeability? At the beginning of the research of metamaterials, only a few materials studies focused on whether conventional materials have the unique properties of metamaterials, and composites with advantage of integrating multi-component properties provided a convenient method to achieve negative electromagnetic parameters [12,13]. The meta-performance of conventional materials is realized and tailored based on the modulation of chemical composition and microstructure by typical materials preparation methods. Studies of the negative electromagnetic parameters, including negative permittivity and negative permeability, have recently become a research hotspot in the field of materials science, and these relevant studies become important supplements to the research of metamaterials.

Negative permittivity has attracted widespread attention in the optical dielectric function of metals and semiconductors [14,15]. In metamaterials, negative permittivity is essential for the meta-performance like negative refraction, negative phase velocity, reverse Doppler effect and Cerenkov effect, etc. [16–18]. Investigations carried out from the perspective of materials science have revealed that the negative permittivity can be realized in radio-frequency band which is much lower than the optical frequency [19–21]. Materials with negative permittivity are described as epsilon-negative materials (ENMs). ENMs realized by composites are classified as metamaterials, which defines the composites with novel and unique properties that different from other conventional materials [22–24]. Thus, ENMs can be divided into

metamaterials and metamaterials, while metamaterials are classified into ceramic matrix composites and polymer matrix composites according to their different composition. In addition, ENMs also consist of homogeneous ceramics or doped polymers. Moreover, ENMs have shown great potential in various electromagnetic and electronic applications, such as electromagnetic shielding, wave absorbing, laminated capacitors, and coil-less inductors [25–28]. In this paper, the research progress of materials with negative permittivity was reviewed. The research methods, preparation processes, mechanism of negative permittivity, as well as the potential applications for ENMs were outlined from the perspective of materials science.

## 2 Realization of epsilon-negative materials

### 2.1 Metamaterials for ENMs

In 1968, V. G. Veselago firstly envisaged the substances with simultaneous negative permittivity and negative permeability, and expounded the rule of propagation for electromagnetic wave in media with negative electromagnetic parameters [17]. Until 1996, J. B. Pendry proposed metallic mesostructures that constructed by thin metal wires to realize the negative permittivity in GHz bands [6]. In fact, metals exhibit plasma behaviors under the action of electromagnetic waves, and of which the frequency dependence of permittivity is described as [4]:

$$\epsilon = 1 - \frac{\omega_p^2}{\omega^2 - j\omega\gamma} \quad (1)$$

where  $\omega_p$  is the plasma frequency, which is determined by the effective electron concentration ( $n_{\text{eff}}$ ) and effective mass ( $m_{\text{eff}}$ ) of electrons.  $\gamma$  is the damping factor that represents the dissipation of energy into system. For simple metals,  $\gamma$  is much smaller than  $\omega_p$ , so it can be considered that the sign of permittivity is mainly determined by plasma frequency that given by  $\omega_p = n_{\text{eff}}e^2/m_{\text{eff}}\epsilon_0$ . Generally,  $\omega_p$  of common metals is in ultraviolet band, and the permittivity is usually negative when frequency is below  $\omega_p$ . With frequency decreasing, the real part of permittivity decreases rapidly and simultaneously the imaginary part increases dramatically. In Pendry's work, the realization of negative permittivity in GHz band is based on the array structure of thin metal wires. As shown in Figure 2a, assuming that the thin metal wires with diameter of  $d = 2r$  are arranged into cubic structures, the space between two wires is  $a$ , the effective average concentration ( $n_{\text{eff}}$ ) of this cubic lattice is deduced as:

$$n_{\text{eff}} = n \frac{\pi r^2}{a^2} \quad (2)$$

where  $n$  is the electron concentration in metal wires. Meanwhile, affected by the self-inductance of the wire structure,  $m_{\text{eff}}$  of electrons in the wire arrays is expressed as:

$$m_{\text{eff}} = \frac{\mu_0 \pi r^2 e^2 n}{2\pi} \ln \frac{a}{r} \quad (3)$$

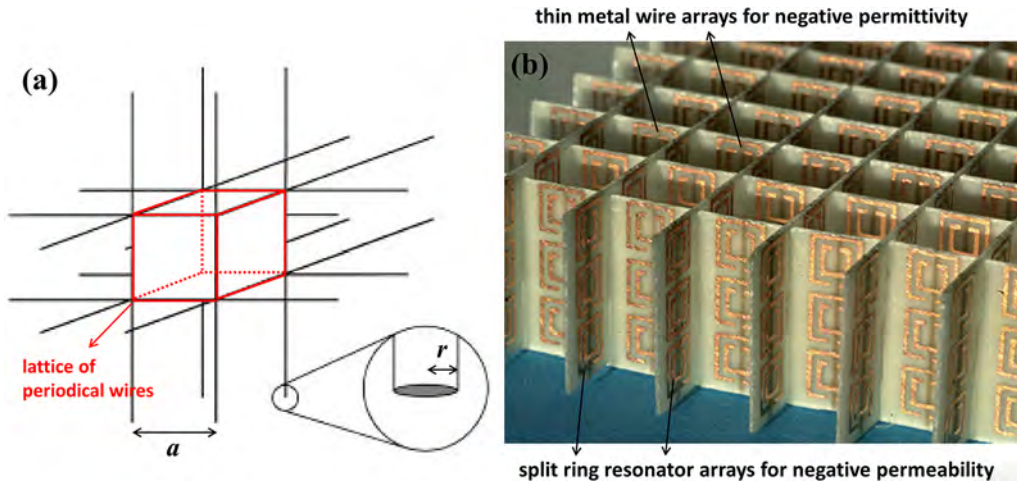


**Fig. 2.** Schematic diagram of lattice of periodic metal wires proposed by J. B. Pendry. (a) [6] Copyright © 1996, American Physical Society; Photograph of metamaterial sample composed of metal wire and split ring resonator arrays by Padilla et al. [18]. (b) Copyright © 2006, Elsevier.

Therefore,  $\omega_p$  of the metal wire array is:

$$\omega_p^2 = \frac{2\pi\mu_0\epsilon_0}{a^2 \ln(a/r)} \quad (4)$$

which is related to the arrangement, the thickness, and the electron concentration of the metal wires. Therefore, the plasma frequency could be shifted to microwave band that is far below than the ultraviolet band and the negative permittivity can be easily tailored through modulating the wire arrays [6]. Afterwards, periodic split ring resonators were introduced and negative permeability was realized due to LC resonance of the induced currents in metal split rings [18,29,30]. The artificial metamaterials are confirmed to be epsilon-negative and mu-negative media that realized on the basis of structural design. Moreover, metamaterials with simultaneous negative permittivity and negative permeability were verified to possess negative refraction and left-hand performance [9,16].

## 2.2 Ceramic matrix composites (CMCs) for ENMs

Composites are composed of two or more different components to obtain novel properties that different from those components [11,31]. The principles of composites preparation provided a more convenient method for designing and realizing various novel properties that are rarely seen in elementary substances. Thus, a variety of versatile composites with improved physical/chemical properties have been developed and widely used in electrical, magnetic, acoustic, optical, thermal, and other applications or devices [32,33]. CMCs are those composites with ceramics as matrix and they possess the advantages of high hardness, high strength, and high wear resistance of ceramics. CMCs composed of metal fillers and high dielectric constant matrix have attracted much attention in the field of dielectrics [34]. Copper (Cu), nickel (Ni), and even molybdenum (Mo) were introduced into dielectric

ceramic (like  $\text{BaTiO}_3$ ) matrix to increase the dielectric constant of the composites, which is of great significance to the development of high dielectric constant materials [35–37]. Generally, dielectric constant of metal/ceramic composites increases with metal content increasing below the percolation threshold, and turns into negative when filler content exceeds the percolation threshold [38,39]. The percolated CMCs with the metal content beyond percolation threshold have been verified to be ENMs in the radio-frequency band, and the negative permittivity is closely associated with the composition and microstructure of CMCs.

Fan et al. proposed a simple impregnation-reduction process to prepare metal/ceramic composites [40–43]. As shown in Figure 3, porous ceramic matrix is impregnated into the solutions of metal precursors, then the dried and calcined ceramics that attached with metal oxides are reduced to obtain elementary metals within the ceramic matrix. The reduction reactions are carried out at several hundred degrees centigrade that is much lower than ceramics' sintering temperature, which have effectively avoided the side reactions between metal fillers and ceramic matrix. The final content of metal fillers in ceramic matrix can be easily tuned via repeating the steps of impregnation and reduction. The microstructure of the composites and morphology of the metal fillers inside the ceramic matrix can be modulated with changing the conditions of reduction reactions. SEM images of some typical morphologies of the metal/ceramic composites prepared by this process are shown in Figure 4. With the increase of metal content, the metal fillers gradually become interconnected and finally form networks within the ceramic matrix. At the same time, the electric and dielectric properties change dramatically. The electric conductivity is obviously enhanced with metal content increasing and the dielectric permittivity changes from positive to negative with the formation of the interconnected metallic networks. The morphologies of the filled



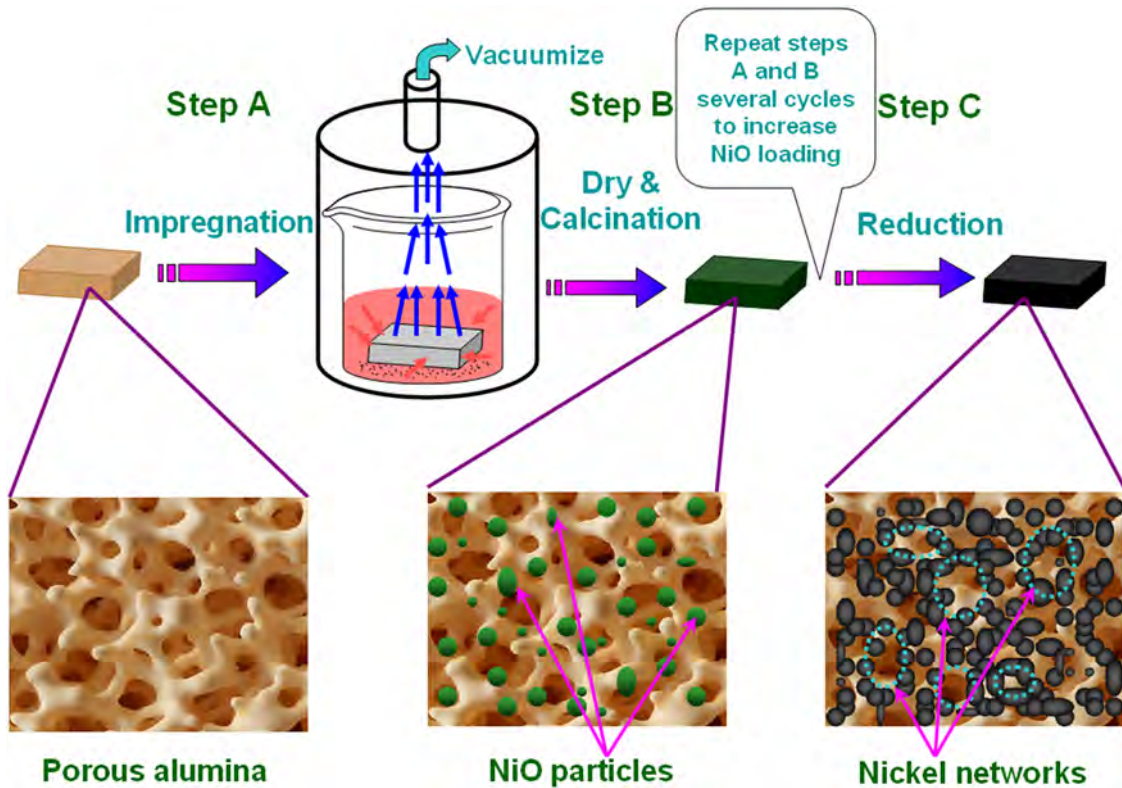


**Fig. 3.** The impregnation-reduction process for the preparation of metal/ceramic composites [40] Copyright © 2012, John Wiley and Sons.

metals are influenced by the different precursor solutions and reduction reactions. The metal fillers can be particles and particle clusters, networks, and flower-like flakes. Therefore, the diversified design of microstructure for the metal/ceramic composites is realized and the epsilon-negative properties is confirmed to be influenced by the composition and microstructure of the composites. Researches in this area have established cases to prepare epsilon-negative materials with composites, and it contributed to the electromagnetic functionalization of conventional structural cermet.

In addition to metal/ceramic composites, multiphase ceramics are also a class of composites that can achieve the epsilon-negative properties. One kind of these ceramics uses conductive ceramics (such as TiN and TiC) and insulating ceramics like  $\text{Al}_2\text{O}_3$  to prepare the ceramic composites, and the other kind selects  $\text{BaTiO}_3$ ,  $\text{SrTiO}_3$ ,  $\text{BiFeO}_3$  and other ferroelectric materials as functional fillers [44–48]. The difference is that the former is similar to metal/ceramic composites, of which the negative permittivity behavior is plasma-like, while the negative permittivity behavior observed in the latter is mainly caused by dielectric resonance. The plasma-like negative permittivity shows negative values in a wide frequency range that below the plasma frequency, while resonance-type negative permittivity only shows negative values in a narrow band near the resonant frequency. As shown in Figure 5, negative permittivity for composites containing ferroelectric components is observed near the resonance frequency.

Negative permittivity in metal/ceramic composites are attributed to plasma oscillations of free electrons, while in the ceramic composites of ferroelectrics, no free electrons are introduced, the resultant epsilon-negative performance is caused by the resonance of dipoles under the action of electric field. Dielectric properties of these ceramic composites are also influenced by composition, from which the frequency band and the strength of the resonance could be regulated in order to realize negative permittivity in a specific frequency range [45,49].

CMCs containing carbonaceous fillers can also be used as advanced electromagnetic materials [50–52]. Carbonaceous materials, such as graphene, carbon fibers, and carbon nanotubes, possessing high electric conductivity, high oxidation resistance, low density and high strength, have been widely used to improve the toughness, strength, and electrical properties of ceramic materials [53–56]. Cheng et al. prepared carbon/silicon nitride ( $\text{Si}_3\text{N}_4$ ) composites by an impregnation-carbonization approach similar to the process shown in Figure 3 [57,58]. The porous  $\text{Si}_3\text{N}_4$  ceramics were impregnated with sucrose aqueous solutions and then carbonized to obtain amorphous carbon within the ceramic matrix. On the one hand, with carbon content increasing, dielectric permittivity of the composites changed from positive to negative. As shown in Figure 6a and b, the pyrolytic carbon gradually becomes interconnected in the ceramic matrix, and the transition of permittivity changing from positive to negative occurs with the evolution of microstructure. The observation of

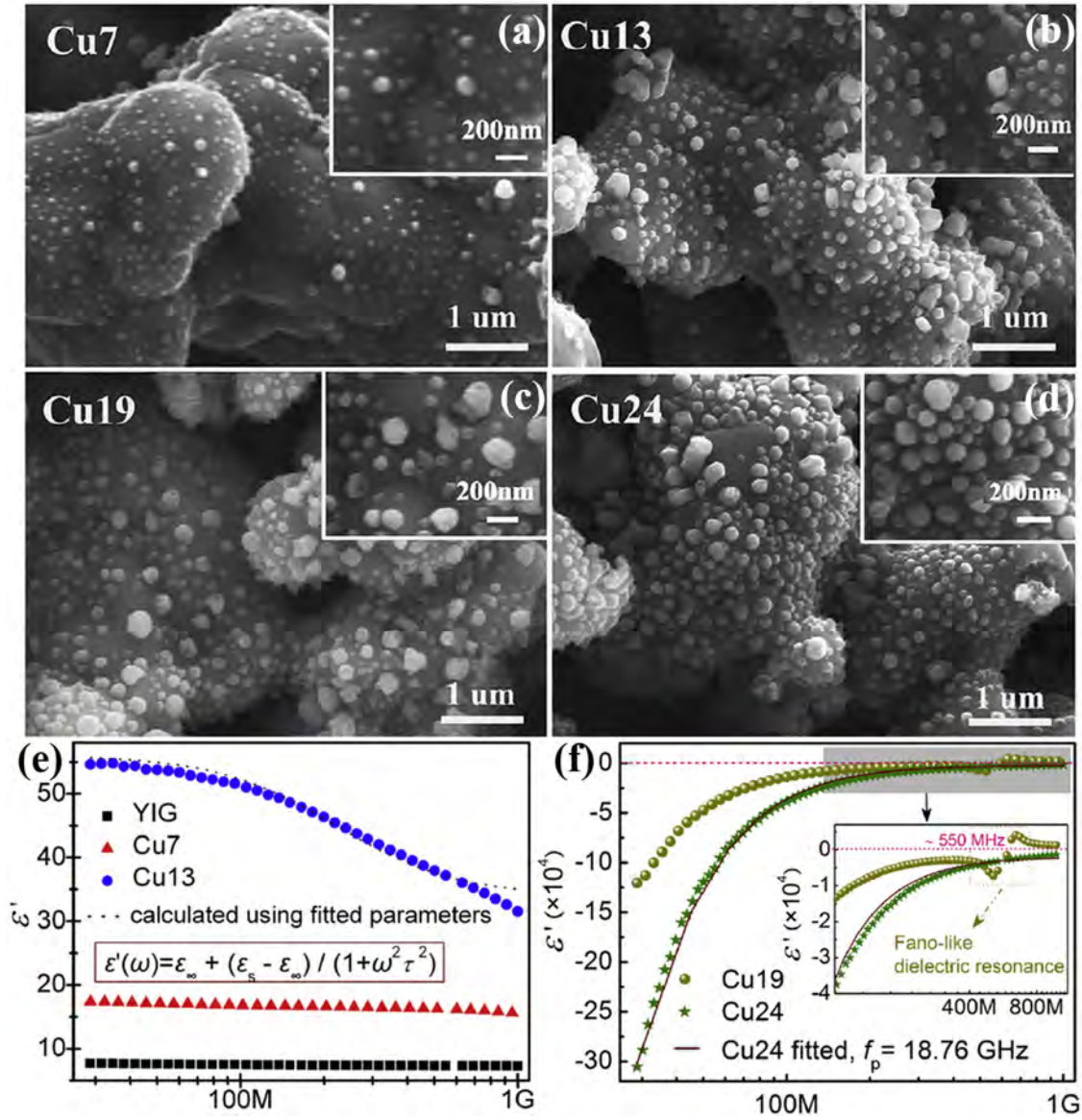


**Fig. 4.** Morphologies and negative permittivity spectra of the metal/ceramic composites prepared impregnation-reduction process. SEM images of Cu/YIG composites with 7 wt% Cu (a), 13 wt% Cu (b), 19 wt% Cu (c), and 24 wt% Cu (d); Permittivity spectra of Cu/YIG composites (e, f) [42] Copyright © 2015, Elsevier.

negative permittivity is attributed to the formed continuous carbon networks in the ceramic matrix. On the other hand, epsilon-negative properties of the C/Si<sub>3</sub>N<sub>4</sub> composites are also influenced by the carbonization temperature. As shown in Figure 6c, the pyrolytic carbon obtained from higher treating temperature possesses higher graphitization degree, with which the highly crystalline carbon clusters forms conductive pathways, leading to the more significant epsilon-negative performance. From this point of view, CMCs with conductive carbon materials as fillers are similar to the metal/ceramic composites, in which the negative permittivity properties are all attributed to the percolating pathways of conductive fillers within the ceramic matrix. In addition, negative permittivity properties have also been studied in some dense ceramics with

graphene, multi-wall carbon nanotubes (MWCNTs) or carbon blacks as fillers [59–62]. It's noteworthy that both resonance-type and plasma-like negative permittivity spectra were observed in MWCNTs/Al<sub>2</sub>O<sub>3</sub> composites. The induced electric dipoles in isolated MWCNTs caused the dielectric resonance for composites with low filling content, and the formed conductive networks of MWCNTs within insulating Al<sub>2</sub>O<sub>3</sub> matrix resulted in the plasma-like negative permittivity behavior, similar phenomena have been also observed in some metal/ceramic composites [38]. Moreover, it's interesting to find that negative permittivity of CMCs with carbonaceous fillers hold smaller absolute values than that of metal/ceramic composites, which may be related to the moderate carrier concentration of the carbonaceous fillers [58,63]. In short, CMCs provide

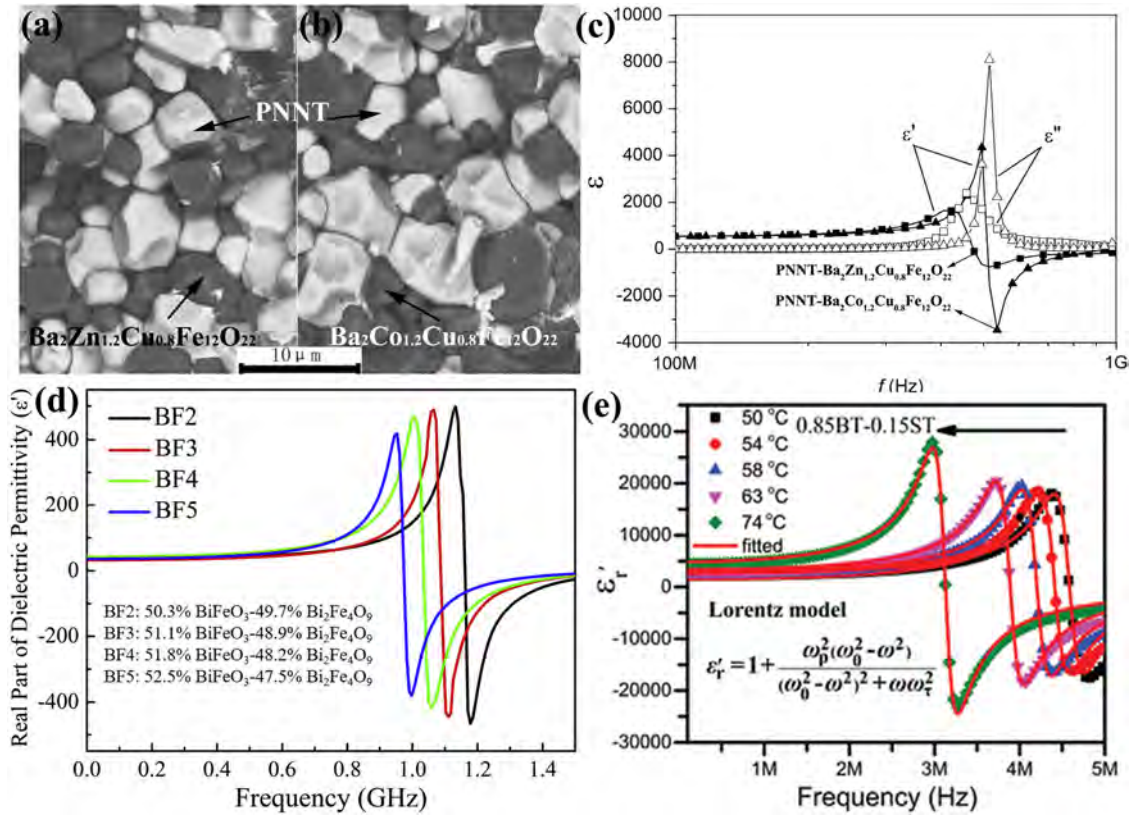


**Fig. 5.** Morphologies and dielectric resonance spectra of multiphase ceramics. SEM images of ceramic composites of  $0.8\text{Pb}(\text{Ni}_{1/2}\text{Nb}_{2/3})\text{O}_3\text{-}0.2\text{PbTiO}_3(\text{PNNT})/\text{Ba}_2\text{Zn}_{1.2}\text{Cu}_{0.8}\text{Fe}_{12}\text{O}_{22}$  (a), and  $\text{PNNT}/\text{Ba}_2\text{Co}_{1.2}\text{Cu}_{0.8}\text{Fe}_{12}\text{O}_{22}$  (b); Permittivity spectra of  $\text{PNNT}/\text{Ba}_2\text{Zn}_{1.2}\text{Cu}_{0.8}\text{Fe}_{12}\text{O}_{22}$  composites (c) [46] Copyright © 2006, AIP Publishing; Permittivity spectra of  $\text{BiFeO}_3/\text{Bi}_2\text{Fe}_4\text{O}_9$  composites (d) [47] Copyright © 2018, Elsevier; Permittivity spectra of  $\text{BaTiO}_3/\text{SrTiO}_3$  composites (e) [48] Copyright © 2019, John Wiley and Sons.

an alternative for the preparation of epsilon-negative materials, of which the negative permittivity can be tailored by the research methods of materials science.

### 2.3 Polymer matrix composites (PMCs) for ENMs

PMCs are composites with polymer materials as matrix, and the functional fillers can be carbonaceous materials, polymers, metals, and ceramics [65–67]. Similar to CMCs, negative permittivity could also be realized in PMCs with enough conductive fillers. Compared with ceramic matrix, polymer materials as matrix could make PMCs flexible and stretchable [68]. Sun et al. fabricated MWCNTs/PDMS composites with a simple tape casting method [69]. As shown in Figure 7a–d, due to the large aspect ratio of MWCNTs, negative permittivity is observed in the composites with only 5 wt% MWCNTs owing to the very low percolation threshold, and graphene as fillers also makes the PDMS composites show negative permittivity at very low filling content [70]. A more convenient process of mixing and curing was used to prepare PVA matrix composites, as shown in Figure 7e and f, the filling of graphene or conductive carbon fibers ensures the composites show out epsilon-negative performance [71,72]. The composites with PDMS or PVA as matrix are flexible and stretchable despite the addition of carbonaceous fillers,

which makes the polymer matrix-ENMs have potential application in some wearable devices. PMCs with negative permittivity have more design possibilities. The epsilon-negative properties realized with Ag-nanowires/polyurethane sponge was influenced by the elastic deformation of polymer matrix, suggesting the compressible ENMs may be used as deformation sensors by testing the variation of negative permittivity versus to the applied external force [73]. The epsilon-negative performance of PMCs has been realized in kHz, MHz, and GHz frequency bands, polymer composites with negative permittivity are gradually becoming a new branch of epsilon-negative metamaterials [74–76].

The preparation of PMCs usually doesn't involve a high-temperature sintering process, so the reactions are relatively mild. Therefore, epsilon-negative performance of the PMCs can be easily tailored with the modification of the functional fillers. In P. Xie's works, negative permittivity is realized with epoxy-based composites with Fe and Fe-alloy particles as conductive fillers [77,78]. The epsilon-negative properties are attributed to the percolating networks formed by interconnected metal particles. Then they proposed a method to tailor negative permittivity via coating the conductive fillers with insulating  $\text{SiO}_2$ . As shown in Figure 8, when the fillers of PMCs are both bare and coated metal particles, the coated fillers would cut off



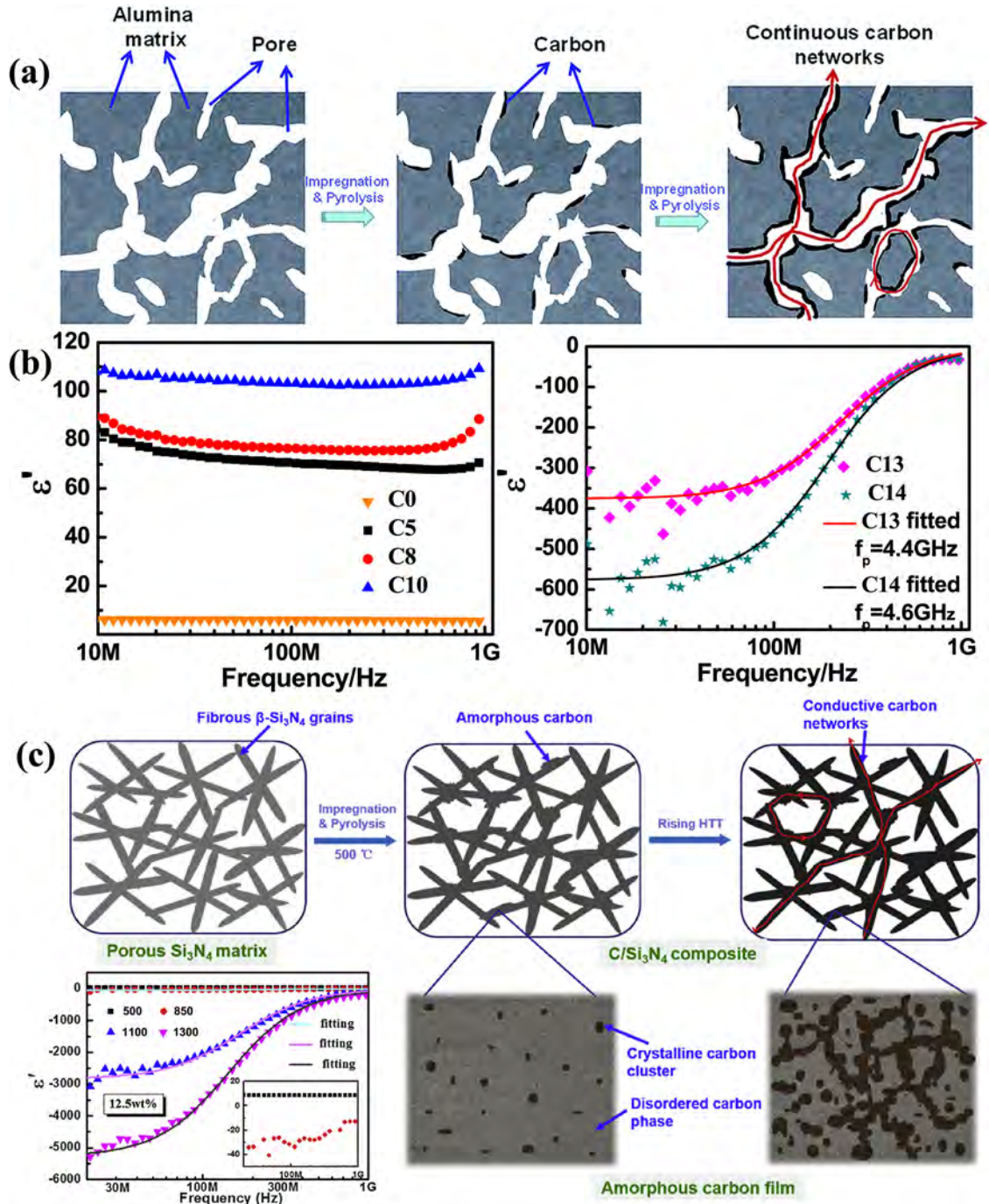


**Fig. 6.** CMCs containing carbonaceous fillers for epsilon-negative metacomposites. Schematic preparation process (a) (Copyright © 2016, The Royal Society of Chemistry) and permittivity spectra (b) (Copyright © 2016, Elsevier) of C/Si<sub>3</sub>N<sub>4</sub> composites with different carbon content [57,64]; Schematic diagram of microstructure and permittivity spectra of C/Si<sub>3</sub>N<sub>4</sub> composites carbonized at different temperature (c) [58] Copyright © 2017, Elsevier.

the interconnected networks, leading to effective electron concentration of the composites changed. As a result, the absolute values and frequency dispersion of the negative permittivity are both influenced by the addition of coated particles. With the increase of coated fillers, negative permittivity decreases and at same time the frequency point for permittivity changing from negative to positive shifted to low frequency. The coated particles are electric

capacitive ( $C$ ) and the interconnected bare particles are inductive ( $L$ ), as a result, negative permittivity of these ternary composites are influenced by  $LC$  resonance [78]. In addition, influence of the synergistic effect of 1-dimensional CNTs and 2-dimensional graphene flakes on the epsilon-negative properties of phenolic resin composites have also been investigated, suggesting the addition of CNTs is beneficial to the appearance of negative permittivity for the

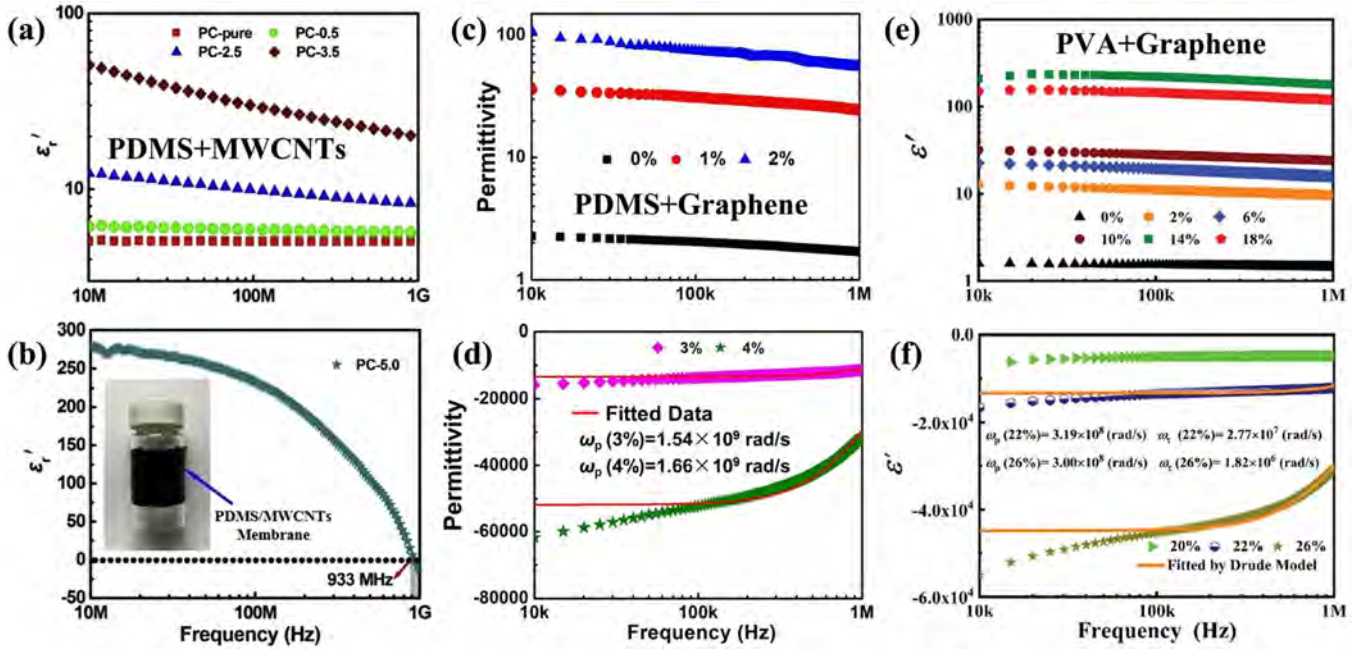


**Fig. 7.** Flexible PMCs for epsilon-negative metamaterials. Permittivity spectra of MWCNTs/PDMS composites (a, b) [69] Copyright © 2017, Elsevier; Permittivity spectra of graphene/PDMS composites (c, d) [70] Copyright © 2019, American Chemical Society; Permittivity spectra of graphene/PVA composites (e, f) [71] Copyright © 2020, John Wiley and Sons.

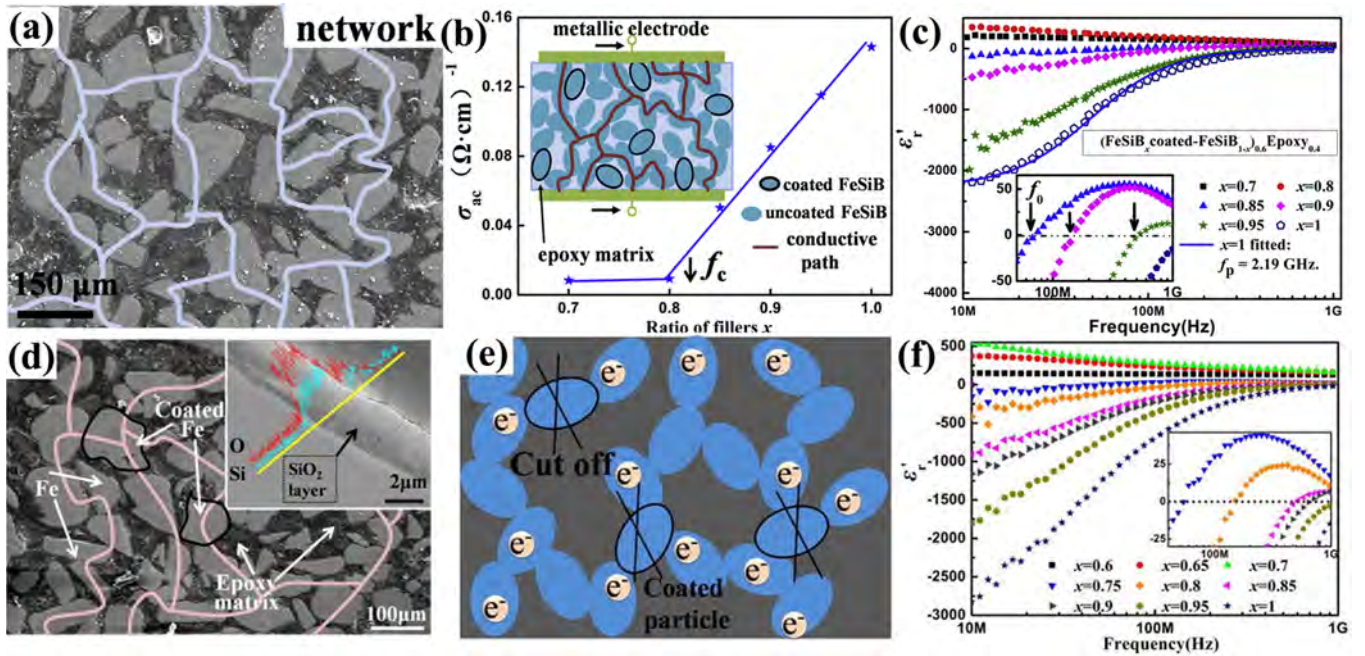


**Fig. 8.** Microstructure (a), electric conductivity (b), and permittivity spectra (c) of  $(\text{FeSiB}_x\text{-coated-FeSiB}_{1-x})_{0.6}\text{Epoxy}_{0.4}$  [77] Copyright © 2017, Elsevier; Microstructure (d), schematic diagram of the microstructure (e), and permittivity spectra (f) of  $(\text{Fe}_x\text{-coated-Fe}_{1-x})_{0.7}\text{Epoxy}_{0.3}$  [78] Copyright © 2017, AIP Publishing.

ternary composites [79]. The modification of conductive fillers or the introduction of another conductive component aims to tailor the microstructure of PMCs in order to modulate the epsilon-negative properties [80].

Thus it can be seen that the processes commonly used to prepare CMCs and PMCs can be employed to prepare the epsilon-negative materials by adding conductive fillers. The modulation of negative permittivity of the composites



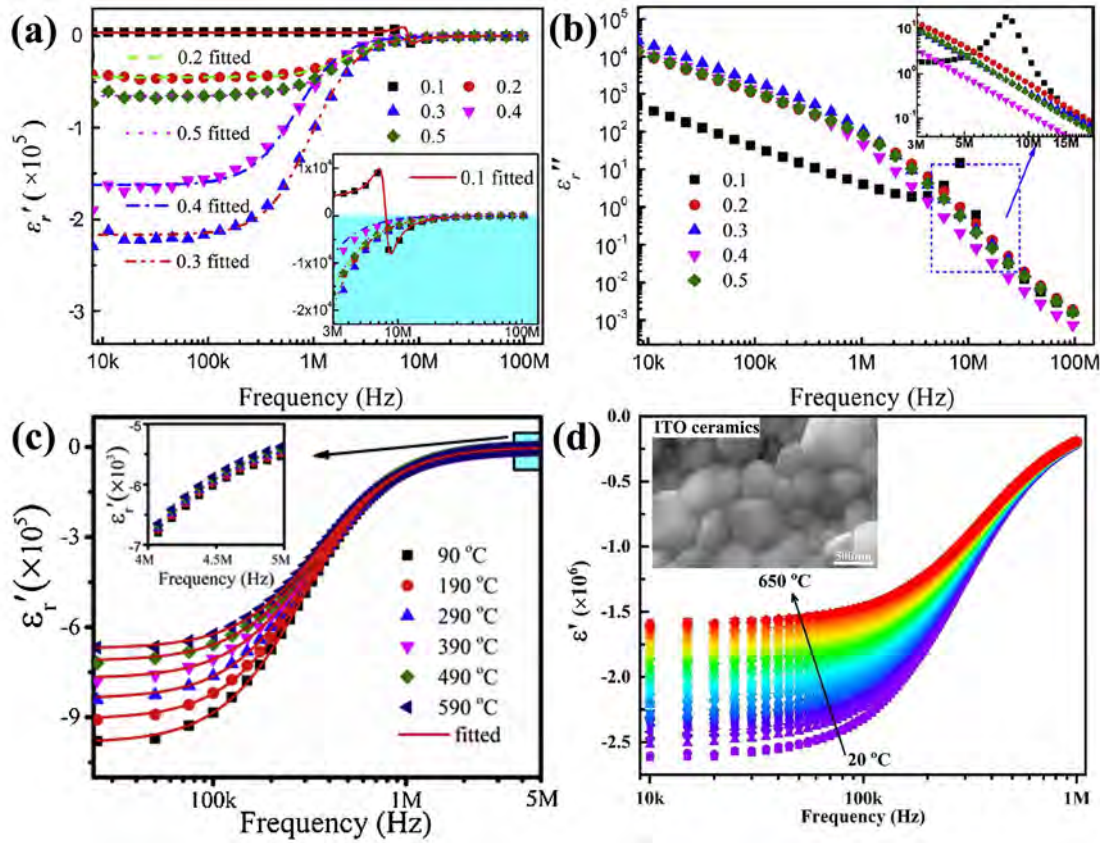


**Fig. 9.** Negative permittivity of doped ceramics. (a, b) Frequency dependence of the real and imaginary part of permittivity for  $\text{La}_{1-x}\text{Sr}_x\text{MnO}_3$  ( $x = 0.1, 0.2, 0.3, 0.4, 0.5$ ) ceramics [81] Copyright © 2015, Elsevier; (c) Negative permittivity spectra of  $\text{La}_{0.5}\text{Sr}_{0.5}\text{MnO}_3$  ceramics at different temperature [83] Copyright © 2020, Elsevier; (d) Negative permittivity spectra of tin-doped indium oxide ceramics at different temperature [85] Copyright © 2021, Elsevier.

can be achieved through composition design and microstructure adjustment, which is in line with the research method and standpoint of materials science. Compared with ceramic-based ENMs, the preparation process of polymer-based ENMs is much simpler and more diverse. The prepared composites can be not only blocks, but can also flexible films or sheets, which greatly enriches the diversity of ENMs.

## 2.4 Doped ceramics or polymers for ENMs

It can be considered that the functional components are ordered in metamaterials, while the conductive fillers in composites are random and disordered. Except for the negative permittivity accompanied with dielectric resonance, appearance of the plasma-like negative permittivity behavior in CMCs and PMCs is closely related to the formed conductive networks in the insulating matrix. From another perspective, the epsilon-negative property of composites is realized by regulating the effective electron concentration. The thin metal wire arrays could be considered as that the metal block has been substantially diluted. Similarly, CMCs and PMCs could also be regarded as that the extensive free electrons within them are diluted by the insulating matrix. From this it appears that the

appropriate electron concentration is of great significance to the realization of negative permittivity, which seems to be independent of whether the electrons are uniformly distributed in the material. Therefore, some mono-phase ceramics and homogenous polymers have been doped to increase electron concentration in order to achieve the epsilon-negative performance.

One kind of the materials that could effectively change electron concentration by doping is semi-metallic materials. Using sol-gel process and auto-combustion methods, Yan et al. prepared Sr-doped  $\text{LaMnO}_3$  ( $\text{La}_{1-x}\text{Sr}_x\text{MnO}_3$ ,  $x = 0.1, 0.2, 0.3, 0.4, 0.5$ ) and studied the electric and dielectric properties [81,82]. Due to the double-exchange effect, electron concentration and electric conductivity of the doped  $\text{La}_{1-x}\text{Sr}_x\text{MnO}_3$  ceramics are evidently improved, and the dielectric properties are also influenced by Sr-doping. As shown in Figure 9a and b, as Sr-dopants increase from 0.1 to 0.5, dielectric resonance and negative permittivity are both observed. With the increasing of Sr-doping, the absolute values of negative permittivity increase, which is attributed to the increased electron concentration caused by Sr-doping. In addition, it can be observed the doped ceramics exhibit evident dielectric loss with the appearance of negative permittivity. For  $x = 0.1$ , the loss peak of dielectric resonance is observed;

for the case of  $x$  varying from 0.2 to 0.5, the imaginary part of permittivity decreases with frequency increasing, suggesting the dielectric loss is mainly caused by conducting loss. Wang et al. studied the negative permittivity performance in  $\text{La}_{0.5}\text{Sr}_{0.5}\text{MnO}_3$  ceramics at different temperature, as shown in Figure 9c [83]. The results show that the plasma-like negative permittivity behavior is temperature-dependent. With temperature increasing, variation trends of the negative permittivity spectra are almost unchanged, while the absolute values of negative permittivity decrease, which is caused by that the plasmonic state of free electrons is affected by the elevated temperature. Free electrons obtain higher energy and move faster yet more randomly at high temperature due to the more significant scattering effect, leading to the plasma oscillation process can not be excited as effectively as at low temperature [84]. Another promising kind of materials that could realize epsilon-negative properties by doping is semiconductors, of which the electron concentration can be easily improved via donor dopants doping. Tin-doped indium oxide (ITO) and antimony-doped tin oxide (ATO) have been successively investigated for single phase epsilon-negative ceramics [85,86]. As shown in Figure 9d, epsilon-negative performance is realized and the temperature-dependent negative permittivity is like that in semi-metallic materials. Epsilon-negative behavior originates from the plasmonic state of free electrons and the decreasing negative permittivity is ascribed to the increased scattering effect with temperature increasing. In addition to semi-metallic materials and semiconductors, Bi-based perovskite structured superconducting material,  $(\text{Bi}_{0.3}\text{Eu}_{0.7})\text{Sr}_2\text{CaCu}_2\text{O}_{6.5}$  ceramic, has been also studied for ENMs, of which the negative permittivity is attributed to plasma oscillations and could be tuned by some rare earth elements doping [87].

The doping-dependent negative permittivity is also observed in homogeneous polymers. For some conducting polymers, such as polypyrrole (PPy) and polyaniline (PNAI), the electric conductivity can be effectively improved by doping with specific types of ions. Investigations on the hexafluorophosphate doped PPy and d, 1-camphorsulfonic acid doped PANI have suggested that delocalized electrons are introduced with doping and the polymers with high electron concentration change into metallic state from insulator [88,89]. As a result, negative permittivity has also been realized with these conducting polymers as the frequency varies from kHz to GHz, even to THz and optical bands [90–93]. As shown in Figure 10a, Xu et al. doped PANI with different acid. The crystallinity of PANI is improved after doping, which is conducive to the electrons transport between molecular chains. Negative permittivity appears due to the plasma oscillations of free electrons. Meanwhile, the epsilon-negative properties are different due to the influence of different acid are different on the structure of PANI. In addition, Figure 10b shows negative permittivity doped with PTSA is affected by its doping amount, which is attributed to that electron concentration is related to acid amount [90]. Phosphoric acid ( $\text{H}_3\text{PO}_4$ ) doped poly (benzimidazole) (PBI) also shows negative permittivity as temperature increases, as shown in Figure 10c. With temperature increasing, the permittivity

is increased due to the higher polarization of the doped ions with higher mobility at high temperature. The permittivity decreases with increasing frequency, exhibiting relaxation and resonance dispersion. With the appearance of resonance, the permittivity has undergone a transition from positive to negative [94]. The epsilon-negative properties are also affected by the orientation of polymers, as shown in Figure 10d, negative permittivity of the hexafluorophosphate (PF6)-doped polypyrrole (PPy) is different at the direction parallel or perpendicular to the orientation [93]. In addition to these doped polymers, some other homogeneous polymers are developed to be ENMs via injecting static charges. Similarly, the negative permittivity is attributed to the plasmonic state of the charges in electric field [28].

## 2.5 Mechanism of negative permittivity in ENMs

The dielectric permittivity reveals the response modes and abilities of the electric charges of materials to an exerted electric field. For composites consist of conductive fillers and insulator matrix, the permittivity is positive when filler content is low. In this case the homogeneously distributed fillers are isolated within the insulating matrix. Interfacial polarizations are increased with filler's content increasing, leading to the permittivity of composites increases [95,96]. As the conductive filler's content further increases and exceeds the percolation threshold, physical properties of the composites would be dramatically changed. In this case the content of conductive fillers is high enough to form the percolating pathways, resulting in electric conductivity of composites increases substantially and permittivity turns into negative values from positive [97,98]. The epsilon-negative properties of composites are closely related to the formed percolating networks of the interconnected conductive fillers. When the composites are put into an electric field, the extensive delocalized electrons would be accelerated under the action of electric field force and then be drawn backward by the coulombic force exerted by positive ion cores. Such a repeated motion process of electrons in alternating electric field is considered as plasma oscillations [99,100]. It's widely accepted that the negative permittivity behavior derived from plasmonic state of free electrons is plasma-like, the real part of permittivity that deduced from the Drude model of equation (1) is represented as below [23,101]:

$$\varepsilon' = 1 - \frac{\omega_p^2}{\omega^2 + \gamma^2}. \quad (5)$$

For composites containing conductor fillers, the plasma frequency  $\omega_p$  is determined by the content of conductor fillers due to free electrons in these heterogeneous composites are mainly introduced in this way. The composites with different content of conductors can be considered as the extensive electrons are diluted by insulating ceramic or polymer matrix in different degree, similar to the idea of wire arrays in metamaterials. The epsilon-negative properties of the percolative conductor/insulator composites therefore can be tailored through the regulation of composition [102,103]. When dielectric



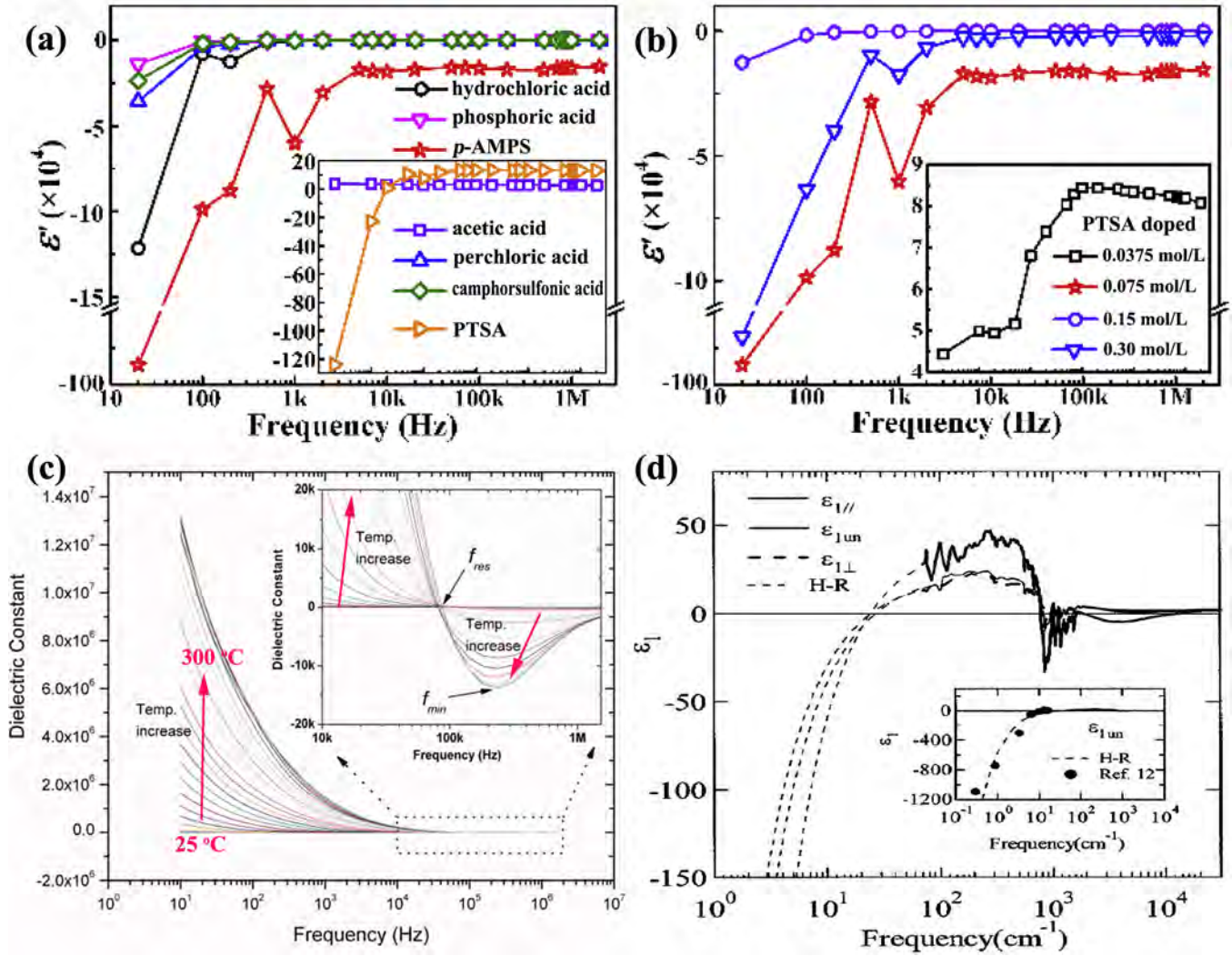


**Fig. 10.** Negative permittivity in various doped-polymers. PANI doped with different acids (a), PANI doped with PTSA with different concentration (b) [90] Copyright © 2020, Elsevier; PBI doped with  $H_3PO_4$  (c) [94] Copyright © 2012, John Wiley and Sons; PPy doped with  $PF_6$  (d) [93] Copyright © 2003, American Physical Society.

resonance is induced in the dielectric components or the isolated conductor fillers of composites, epsilon-negative properties could be also realized. In this case the negative permittivity appears only in a narrow range near the resonance frequency. The resonance-type negative permittivity behavior can be well described by Lorentz model [48,104]:

$$\epsilon' = 1 + \frac{\omega_p^2(\omega_0^2 - \omega^2)}{(\omega_0^2 - \omega^2)^2 + \omega^2\Gamma_1^2}. \quad (6)$$

Figure 11a and b shows the mechanism of negative permittivity in composites can be attributed to dielectric resonance and the plasmonic state of free electrons induced in the percolating pathways [105]. Sometimes the resonance-type and plasma-like negative permittivity behavior can also be observed at the same time, as shown in Figure 11c. For the composites with conductor fillers content close to percolation threshold, resonance response

of isolated particles and plasmonic state induced in the connected networks can be realized simultaneously, resulting in the complicated permittivity spectra, that can be explained by combining the Drude model and Lorentz model [106,107]. Therefore, materials with tunable negative permittivity could be obtained by the means of the preparation process of composites. The homogeneous materials of ceramics or polymers are also promising for ENMs as long as free electrons with appropriate concentration is introduced. The plasma frequency could be regulated to shift from several kHz to GHz and even optical bands by regulating average electron concentration, thus negative permittivity could be tailored in a very wide frequency band. Compared to the wire arrays with periodic structure, the various materials with negative permittivity in the above review are all prepared with the method of material science, which not only expands the concept of ENMs, but also enriches the connotation of advanced functional materials.

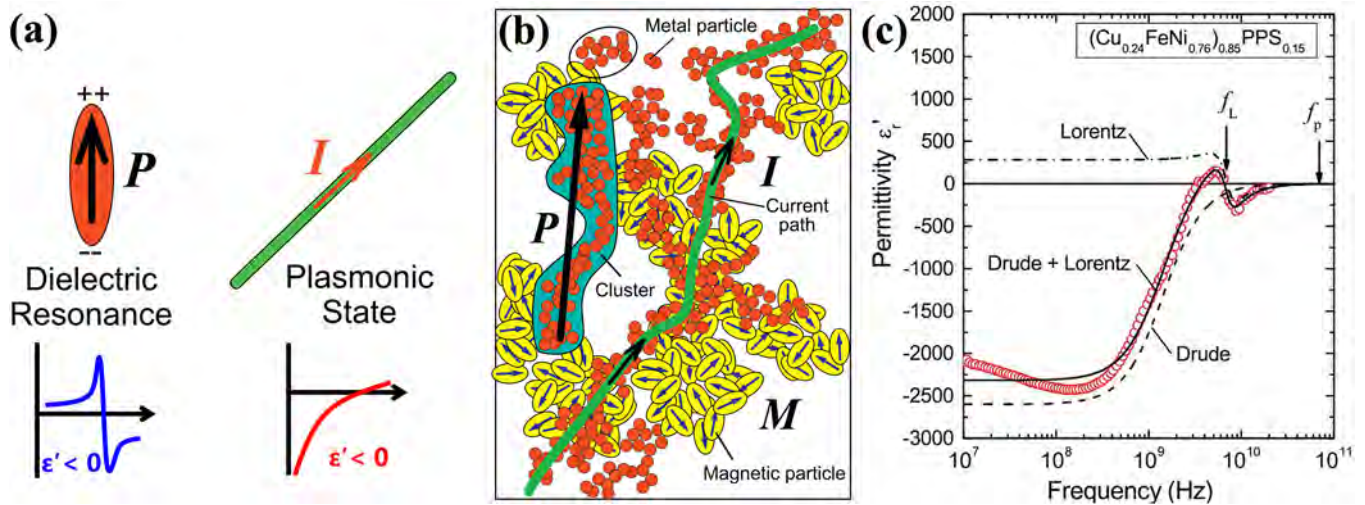


**Fig. 11.** Mechanism of negative permittivity (a) and schematic diagram of the microstructure (b) for epsilon-negative composites [105] Copyright © 2015, Elsevier; (c) shows simultaneous Drude-type and Lorentz-type negative permittivity spectra of  $(\text{Cu}_{0.24}\text{FeNi}_{0.76})_{0.85}\text{PPS}_{0.15}$  composites [106] Copyright © 2016, AIP Publishing.

### 3 The application of epsilon-negative metacomposites

#### 3.1 Electromagnetic interference shielding of ENMs in GHz bands

It's one of the most promising applications for ENMs to be used as novel electromagnetic materials. In past several years, many studies on the applications of ENMs in this field have been carried out. It's found that negative refraction could be realized in ENMs with simultaneous negative permeability. Therefore, the left-handed propagation of electromagnetic waves is expected and the ENMs could be used as high-effective absorbers on condition that impedance matching is satisfied in the ENMs [105,106].

In addition, ENMs composed of CMCs or PMCs were found to exhibit remarkable electromagnetic interference shielding performance in microwave bands. Wu et al. fabricated graphene foam (GF)/poly (3,4-ethylenedioxythiophene): poly (styrenesulfonate) (PEDOT:PSS) composites and investigated the electromagnetic properties in X-band [25]. The results show that negative permittivity is caused by the extensive macroscopically delocalized electrons in the interconnected conductive networks of GFs and highly conductive PEDOT:PSS coatings. As shown in Figure 12a, the absolute values of negative permittivity are increased with the increasing mass ratio of PEDOT:PSS to GF. Figure 12b shows the electromagnetic shielding performance is contributed by absorption and reflection. The former is ascribed to the direct absorption-caused by polarization and multiply reflections, the latter is attributed to interactions between the incident waves and free electrons of materials. The epsilon-negative composites with internally formed three-dimensional conductive networks are taken as loss left-handed materials, and the incident waves would be effectively attenuated without internal propagation. Thus, with the electric

conductivity increases, the shielding effectiveness of absorption ( $SE_A$ ) increases while the shielding effectiveness of reflection ( $SE_R$ ) keeps virtually unchanged, as shown in Figure 12c. Furthermore, Figure 12d and e suggests that  $SE_A$  plays a dominant role in the total shielding effectiveness ( $SE_T$ ), and the composites of GF/PEDOT:PSS-4.6 exhibits high average  $SE_T$  of 91.9 dB, which is much higher than the minimum requirement of 20 dB for commercial applications [108]. What's more attractive is that the graphene nanosheet reinforced  $\text{Al}_2\text{O}_3$  ceramics show temperature-dependent epsilon-negative performance, leading to the ENMs with variable negative permittivity are potential for electromagnetic shielding applications at high temperature [109]. Besides, unlike the absorption dominated shielding effectiveness [108,109], Cheng et al. found the shielding performance of epsilon-negative Ag/ $\text{Si}_3\text{N}_4$  composites are dominated by strong reflection caused by intense impedance mismatching due to the huge values of negative permittivity [110]. These works endowed the electromagnetic functional materials with new choices and provided a novel solution for ENMs to be applied in electromagnetic shielding field.

#### 3.2 Dielectric enhancement in laminated composites containing ENMs

If the considered frequency range is extended to MHz and even kHz bands, the investigations of ENMs will intersect with that of dielectrics. The investigations of dielectrics focus on polarization, and the goal is to achieve high dielectric constant, low dielectric loss and high energy storage density, while most investigations of ENMs are devoted to achieve the tunable negative permittivity based on plasma oscillations of delocalized electrons in the composites [111,112]. It's full of interest to design high permittivity dielectrics with ENMs contained. Based on the capacitance series model, Shi et al. pioneered in the



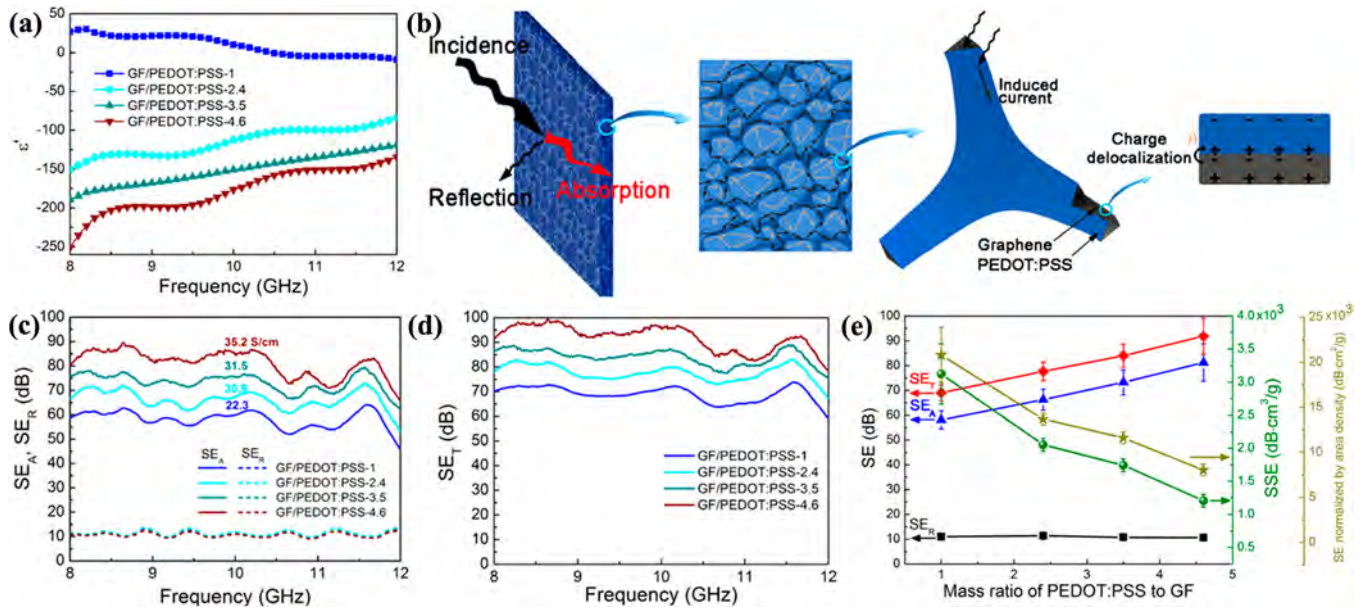


**Fig. 12.** Electromagnetic shielding performance of epsilon-negative GF/PEDOT:PSS composites. Permittivity spectra (a), schematic illustration of the electromagnetic shielding mechanism (b), Shielding effectiveness of absorption ( $SE_A$ ) and reflection ( $SE_R$ ) (c), Total shielding effectiveness ( $SE_T$ ) (d), Summary of SEs, SSEs, and SSEs normalized by area density versus to the mass ratio of PEDOT:PSS to GF (e) [25] Copyright © 2017, American Chemical Society.

investigation of laminated composites containing ENMs layers for high permittivity dielectrics [113,114]. When the permittivity of ENMs layers is balancing by that of dielectrics layers, the laminated composites will exhibit very high dielectric permittivity. As shown in Figure 13a–e, permittivity of bilayer composites composed of one positive- $k$  layer and one negative- $k$  layer represents an increasing tendency with the increase of the thickness ratio of the two layers, while the low dielectric loss is basically unchanged. In addition to the high permittivity and low dielectric loss, high breakdown strength is also essential for the composites to achieve high energy density. Thus, sandwich-structured composites with ENMs as intermediate layer are developed, as shown in Figure 13f, the outer dielectric layers containing  $\text{BaTiO}_3$  fillers are of vital importance to ensure the laminated composites keep low dielectric loss and high breakdown strength. Furthermore, as shown in Figure 13g, Gu et al. introduced both ENMs and insulator layers into the laminated composites to further restrict the dielectric loss and guarantee the high breakdown strength [115]. The extensive delocalized electrons in ENMs and the increased heterogeneous interfaces are favorable to the interfacial polarizations, leading to the enhanced dielectric permittivity. Meanwhile, dielectrics layers confined electrons move in long distance, avoiding the dielectric loss caused by conduction loss. And the insulator layers with high breakdown resistance effectively ensured the composites can not be broken down as the exerted voltage increases. Therefore, the laminated composites containing ENMs layers bring a new approach to the development of novel capacitors.

### 3.3 Other potential applications

The various novel behaviors of ENMs are providing more and more fresh ideas for the design of electronic devices and electromagnetic functional materials. The impedance behaviors of ENMs have been thoroughly discussed in many literatures, demonstrating that the current phase in ENMs lags the voltage phase, which differs from the phase relationships of current and voltage in normal dielectrics [116,117]. Common materials with positive permittivity exhibit capacitance behaviors, and correspondingly, it could be asserted that ENMs with reverse phase relations are electric inductive [28,118]. Inspired by the typical structures of parallel-plate capacitors, Engheta and Li replaced the dielectrics between metal electrodes with an epsilon-negative waveguide structure, resulting in the artificial construct functions with inductive impedance [119]. Therefore, it's promising for ENMs to be applied into coil-less inductors, which is significant to the miniaturization and thin slicing of electric inductors. In addition, it's widely accepted that the plasma-like negative permittivity will turn into positive values as frequency reaches up to plasma frequency. As discussed in former sections, the plasma frequency of composites is not only determined by fillers' content, but also affected by the intrinsic properties of the conductor fillers. The dielectric dispersion and the transition for permittivity changing from negative to positive could be regulated through fillers' modification. From this point of view, Qiu et al. constructed graphene/polyolefin elastomer epsilon-near-zero metamaterials, of which the content and the reduction methods of graphene were adjusted to obtain moderate electron concentration,

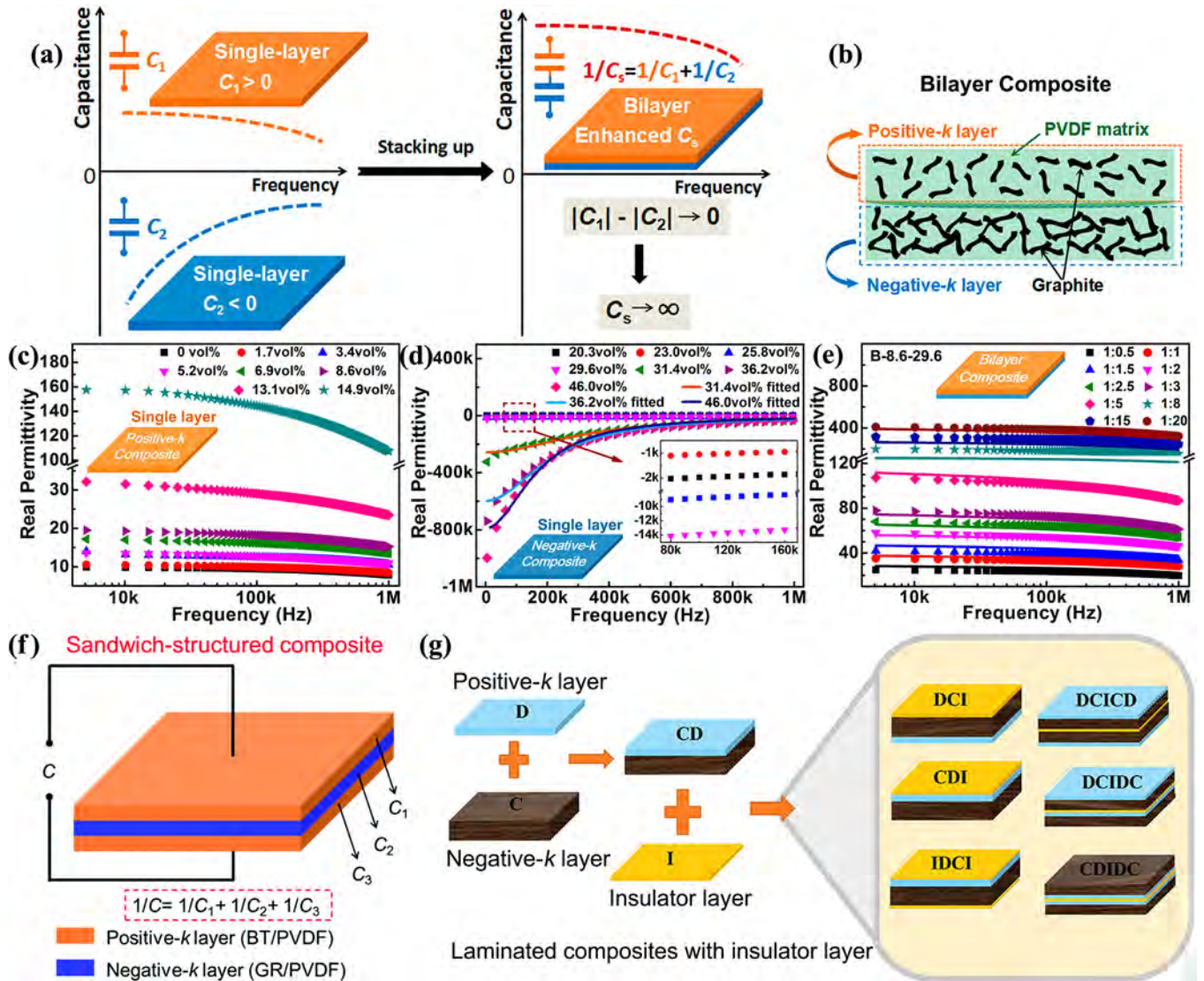


**Fig. 13.** Laminated composites containing ENMs layers for high permittivity dielectrics. Mechanism of dielectric enhancement in bilayer composites with positive- $k$  and negative- $k$  layers (a), Schematic illustration of the bilayer composites (b), Frequency dependence of permittivity of the single layers and bilayer composites (c-e) [113] Copyright © 2017, American Chemical Society; Sandwich-structured composites with positive- $k$ , negative- $k$ , positive- $k$  layers (f) [114] Copyright © 2017, The Royal Society of Chemistry; Multilayered composites containing positive- $k$ , negative- $k$ , and insulator layers (g) [115] Copyright © 2019, American Chemical Society.

resulting in the negative permittivity keeps near-zero in a relatively wide frequency band [120]. ENMs with very small values of negative permittivity are promising for epsilon-negative metamaterials, which will promote the integration of the versatile composites with various metamaterials.

## 4 Summary and outlook

In summary, a compressive review of epsilon-negative materials realized with common composites or homogeneous materials are presented. Negative permittivity will be observed when the plasma oscillation of electrons or the

dielectric resonance of electric dipoles is induced at a certain frequency. Composites with fillers content exceeding percolation threshold are epsilon-negative owing to the three-dimensional connected networks formed by the conductor fillers. The homogeneous ceramics or polymers can also be epsilon-negative, as long as the free electrons within them come into the plasmonic state. The epsilon-negative properties are closely related to the composition and microstructure of various materials. In a word, from the perspective of materials science, various “real” materials even without the precise artificial periodic building blocks of metamaterials can be constructed and regulated to be epsilon-negative materials using materials preparation methods. Moreover, compare to common



positive permittivity materials, epsilon-negative materials have shown great potentials in various electronic and electromagnetic devices due to the completely new response mechanism. The development of the epsilon-negative materials has accelerated the integration of natural materials and metamaterials, and the investigations of epsilon-negative materials are gradually becoming an important branch in the field of metamaterials.

The preparation methods and relation mechanism of epsilon-negative materials with natural materials have been basically clarified, however, in-depth explanations of the mechanism and more abundant means of the property modulation should be further developed in the future work. Researchers working on the epsilon-negative materials may need to cooperate with the peers in the field of dielectrics and metamaterials to further explore the applications in more electronic and electromagnetic devices. At present, the factors that may affect the applications of epsilon-negative materials are still unclear. Therefore, the basic physical properties of these epsilon-negative materials need to be clarified from more aspects. All the efforts made on the various epsilon-negative materials have enriched the connotation of advanced functional materials and metamaterials.

This work was supported by National Natural Science Foundation of China [grant numbers 51771104, 51871146, 51971119], Future Plan for Young Talent of Shandong University [grant number 2016WLJH40], and Innovation Program of Shanghai Municipal Education Commission [grant number 2019-01-07-00-10-E00053].

## References

1. J. Huang, P. Du, L. Hong, Y. Dong, M. Hong, A novel percolative ferromagnetic-ferroelectric composite with significant dielectric and magnetic properties, *Adv. Mater.* **19**, 437 (2007)
2. A.D.M. Charles, A.N. Rider, S.A. Brown, C.H. Wang, Multifunctional magneto-polymer matrix composites for electromagnetic interference suppression, sensors and actuators, *Prog. Mater. Sci.* **115**, 100705 (2021)
3. J. Gou, X. Liu, C. Zhang, G. Sun, Y. Shi, J. Wang, H. Chen, T. Ma, X. Ren, Ferromagnetic composite with stress-insensitive magnetic permeability: compensation of stress-induced anisotropies, *Phys. Rev. Mater.* **2**, 114406 (2018)
4. S.A. Ramakrishna, Physics of negative refractive index materials, *Rep. Prog. Phys.* **68**, 449 (2005)
5. K. Sun, R. Fan, X. Zhang, Z. Zhang, Z. Shi, P. Xie, Z. Wang, G. Fan, N. Wang, C. Liu, T. Li, C. Yan, Z. Guo, An overview of metamaterials and their achievements in wireless power transfer, *J. Mater. Chem. C* **6**, 2925 (2018)
6. J.B. Pendry, A.J. Holden, W.J. Stewart, I.I. Youngs, Extremely low frequency plasmons in metallic mesostructures, *Phys. Rev. Lett.* **76**, 4773 (1996)
7. G. He, R. Wu, Y. Poo, P. Chen, Magnetically tunable double-negative material composed of ferrite-dielectric and metallic mesh, *J. Appl. Phys.* **107**, 093522 (2010)
8. Q. Zhao, J. Zhou, F. Zhang, D. Lippens, Mie resonance-based dielectric metamaterials, *Mater. Today* **12**, 60 (2009)
9. D.R. Smith, W.J. Padilla, D. Vier, S.C. Nemat-Nasser, S. Schultz, Composite medium with simultaneously negative permeability and permittivity, *Phys. Rev. Lett.* **84**, 4184 (2000)
10. Y. Dong, H. Yang, L. Zhang, X. Li, D. Ding, X. Wang, J. Li, J. Li, I.W. Chen, Ultra-uniform nanocrystalline materials via two-step sintering, *Adv. Funct. Mater.* **31**, 2007750 (2020)
11. L.J. Huang, L. Geng, H.X. Peng, Microstructurally inhomogeneous composites: Is a homogeneous reinforcement distribution optimal? *Prog. Mater. Sci.* **71**, 93 (2015)
12. S.T. Chui, L. Hu, Theoretical investigation on the possibility of preparing left-handed materials in metallic magnetic granular composites, *Phys. Rev. B* **65**, 1444071 (2002)
13. J.P. Calame, J. Battat, Narrowband microwave dielectric resonance and negative permittivity behavior in hydrogen-fired  $\text{Al}_2\text{O}_3$ -CuO composites, *J. Am. Ceram. Soc.* **89**, 3865 (2006)
14. P.B. Johnson, R.W. Christy, Optical constants of the noble metals, *Phys. Rev. B* **6**, 4370 (1972)
15. Q. Guo, Y. Cui, Y. Yao, Y. Ye, Y. Yang, X. Liu, S. Zhang, X. Liu, J. Qiu, H. Hosono, A solution-processed ultrafast optical switch based on a nanostructured epsilon-near-zero medium, *Adv. Mater.* **29**, 1700754 (2017)
16. R.A. Shelby, D.R. Smith, S. Schultz, Experimental verification of a negative index of refraction, *Science* **292**, 77 (2001)
17. V.G. Veselago, The electrodynamics of substances with simultaneously negative values of  $\epsilon$  and  $\mu$ , *Sov. Phys. Usp.* **10**, 509 (1968)
18. W.J. Padilla, D.N. Basov, D.R. Smith, Negative refractive index metamaterials, *Mater. Today* **9**, 28 (2006)
19. B. Li, G. Sui, W. Zhong, Single negative metamaterials in unstructured polymer nanocomposites toward selectable and controllable negative permittivity, *Adv. Mater.* **21**, 4176 (2010)
20. T. Tsutaoka, T. Kasagi, S. Yamamoto, K. Hatakeyama, Low frequency plasmonic state and negative permittivity spectra of coagulated Cu granular composite materials in the percolation threshold, *Appl. Phys. Lett.* **102**, 181904 (2013)
21. K. Sun, R. Fan, Z. Zhang, K. Yan, X. Zhang, P. Xie, M. Yu, S. Pan, The tunable negative permittivity and negative permeability of percolative Fe/ $\text{Al}_2\text{O}_3$  composites in radio frequency range, *Appl. Phys. Lett.* **106**, 172902 (2015)
22. A. Neiman, N. Pestereva, A. Sharafutdinov, Y. Kostikov, Conduction and transport numbers in metacomposites  $\text{MeWO}_4 \cdot \text{WO}_3$  (Me=Ca, Sr, Ba), *Russ. J. Electrochem.* **41**, 598 (2005)
23. D. Estevez, F. Qin, Y. Luo, L. Quan, Y. Mai, L. Panina, H. Peng, Tunable negative permittivity in nano-carbon coated magnetic microwire polymer metacomposites, *Compos. Sci. Technol.* **171**, 206 (2019)
24. T. Kasagi, T. Tsutaoka, K. Hatakeyama, Electromagnetic properties of permendur granular composite materials containing flaky particles, *J. Appl. Phys.* **116**, 153901 (2014)
25. Y. Wu, Z. Wang, X. Liu, X. Shen, Q. Zheng, Q. Xue, J.K. Kim, Ultralight graphene foam/conductive polymer composites for exceptional electromagnetic interference shielding, *ACS Appl. Mater. Interfaces* **9**, 9059 (2017)
26. Z. Wang, K. Sun, P. Xie, Y. Liu, Q. Gu, R. Fan, J. Wang, Epsilon-negative  $\text{BaTiO}_3$ /Cu composites with high thermal conductivity and yet low electrical conductivity, *J. Mater. Sci.* **6**, 145 (2020)

27. Z. Wang, J. Fan, X. Guo, J. Ji, Z. Sun, Enhanced permittivity of negative permittivity middle-layer sandwich polymer matrix composites through conductive filling with flake MAX phase ceramics, *RSC Adv.* **1**, 2725 (2020)
28. H. Yan, C. Zhao, K. Wang, L. Deng, M. Ma, G. Xu, Negative dielectric constant manifested by static electricity, *Appl. Phys. Lett.* **102**, 062904 (2013)
29. J.B. Pendry, A.J. Holden, D.J. Robbins, W.J. Stewart, Magnetism from conductors and enhanced nonlinear phenomena, *IEEE Trans. Microwave Theory Tech.* **47**, 2075 (1999)
30. J.B. Pendry, D.R. Smith, Reversing light with negative refraction, *Phys. Today* **57**, 37 (2004)
31. C. Nan, Y. Shen, J. Ma, Physical properties of composites near percolation, *Annu. Rev. Mater. Res.* **40**, 131 (2010)
32. K. Wu, Y. Xue, W. Yang, S. Chai, F. Chen, Q. Fu, Largely enhanced thermal and electrical conductivity via constructing double percolated filler network in polypropylene/expanded graphite-Multi-wall carbon nanotubes ternary composites, *Compos. Sci. Technol.* **130**, 28 (2016)
33. Y. Shen, X. Zhang, M. Li, Y. Lin, C. Nan, Polymer nanocomposite dielectrics for electrical energy storage, *Natl. Sci. Rev.* **4**, 23 (2017)
34. H. Du, X. Lin, H. Zheng, B. Qu, Y. Huang, D. Chu, Colossal permittivity in percolative ceramic/metal dielectric composites, *J. Alloys Compd.* **663**, 848 (2016)
35. N. Xu, Y.P. Pu, Z. Wang, Large Dielectric constant and maxwell-wagner effects in BaTiO<sub>3</sub>/Cu composites, *J. Am. Ceram. Soc.* **95**, 999 (2012)
36. C. Pecharroman, F. Esteban-Betegon, J.F. Bartolome, S. Lopez-Esteban, J.S. Moya, New percolative BaTiO<sub>3</sub>-Ni composites with a high and frequency-independent dielectric constant ( $\epsilon_r \approx 80000$ ), *Adv. Mater.* **13**, 1541 (2001)
37. C. Pecharromán, J.S. Moya, Experimental evidence of a giant capacitance in insulator-conductor composites at the percolation threshold, *Adv. Mater.* **12**, 294 (2000)
38. G. Fan, Z. Wang, H. Ren, Y. Liu, R. Fan, Dielectric dispersion of copper/rutile cermets: dielectric resonance, relaxation, and plasma oscillation, *Scr. Mater.* **190**, 1 (2021)
39. G. Fan, Z. Wang, Z. Wei, Y. Liu, R. Fan, Negative dielectric permittivity and high-frequency diamagnetic responses of percolated nickel/rutile cermets, *Compos. Part A* **139**, 106132 (2020)
40. Z. Shi, R. Fan, Z. Zhang, L. Qian, M. Gao, M. Zhang, L. Zheng, X. Zhang, L. Yin, Random composites of nickel networks supported by porous alumina toward double negative materials, *Adv. Mater.* **24**, 2349 (2012)
41. Z. Shi, R. Fan, K. Yan, K. Sun, M. Zhang, C. Wang, X. Liu, X. Zhang, Preparation of iron networks hosted in porous alumina with tunable negative permittivity and permeability, *Adv. Funct. Mater.* **23**, 4123 (2013)
42. Z. Shi, R. Fan, X. Wang, Z. Zhang, L. Qian, L. Yin, Y. Bai, Radio-frequency permeability and permittivity spectra of copper/yttrium iron garnet cermet prepared at low temperatures, *J. Eur. Ceram. Soc.* **35**, 1219 (2015)
43. X. Wang, Z. Shi, M. Chen, R. Fan, K. Yan, K. Sun, S. Pan, M. Yu, Tunable electromagnetic properties in Co/Al<sub>2</sub>O<sub>3</sub> cermets prepared by wet chemical method, *J. Am. Ceram. Soc.* **97**, 3223 (2015)
44. G. Fan, Y. Zhao, J. Xin, Z. Zhang, P. Xie, C. Cheng, Y. Qu, Y. Liu, K. Sun, R. Fan, Negative permittivity in titanium nitride-alumina composite for functionalized structural ceramics, *J. Am. Ceram. Soc.* **103**, 403 (2020)
45. Z. Wang, K. Sun, P. Xie, Y. Liu, R. Fan, Generation mechanism of negative permittivity and Kramers-Kronig relations in BaTiO<sub>3</sub>/Y<sub>3</sub>Fe<sub>5</sub>O<sub>12</sub> multiferroic composites, *J. Phys.: Condens. Matter* **29**, 365703 (2017)
46. Y. Bai, J. Zhou, Y. Sun, B. Li, Z. Yue, Z. Gui, L. Li, Effect of electromagnetic environment on the dielectric resonance in the ferroelectric-ferromagnetic composite, *Appl. Phys. Lett.* **89**, 112907 (2006)
47. Q. Li, S. Bao, Y. Sun, J. Li, Z. Yu, Y. Li, S. Zhang, Y. Liu, Z. Cheng, Tunable dielectric resonance with negative permittivity behavior of BiFeO<sub>3</sub>-Bi<sub>2</sub>Fe<sub>4</sub>O<sub>9</sub> composite at about 1 GHz, *J. Alloys Compd.* **735**, 2081 (2018)
48. Z. Wang, H. Li, H. Hu, Y. Fan, R. Fan, B. Li, J. Zhang, H. Liu, J. Fan, H. Hou, F. Dang, Z. Kou, Z. Guo, Direct observation of stable negative capacitance in SrTiO<sub>3</sub>@BaTiO<sub>3</sub> heterostructure, *Adv. Electron. Mater.* **6**, 1901005 (2020)
49. J.D.L.S. Guerra, J.A. Eiras, Mechanical and electrical driving field induced high-frequency dielectric anomalies in ferroelectric systems, *J. Phys.: Condens. Matter* **19**, 386217 (2007)
50. X. Yin, L. Kong, L. Zhang, L. Cheng, N. Travitzky, P. Greil, Electromagnetic properties of Si-C-N based ceramics and composites, *Int. Mater. Rev.* **59**, 326 (2014)
51. L. Chen, X. Yin, X. Fan, M. Chen, X. Ma, L. Cheng, L. Zhang, Mechanical and electromagnetic shielding properties of carbon fiber reinforced silicon carbide matrix composites, *Carbon* **95**, 10 (2015)
52. J. Ru, Y. Fan, W. Zhou, Z. Zhou, T. Wang, R. Liu, J. Yang, X. Lu, J. Wang, C. Ji, L. Wang, W. Jiang, Electrically conductive and mechanically strong graphene/mullite ceramic composites for high-performance electromagnetic interference shielding, *ACS Appl. Mater. Interfaces* **10**, 39245 (2018)
53. X. Jin, X. Fan, C. Lu, T. Wang, Advances in oxidation and ablation resistance of high and ultra-high temperature ceramics modified or coated carbon/carbon composites, *J. Eur. Ceram. Soc.* **38**, 1 (2018)
54. Y. Dong, L. Ma, C.Y. Tang, F. Yang, X. Quan, D. Jassby, M. J. Zaworotko, M.D. Guiver, Stable superhydrophobic ceramic-based carbon nanotube composite desalination membranes, *Nano Lett.* **18**, 5514 (2018)
55. Q. Zhang, D. Lin, B. Deng, X. Xu, Q. Nian, S. Jin, K.D. Leedy, H. Li, G. Cheng, Flyweight, superelastic, electrically conductive, and flame-retardant 3D multi-nanolayer graphene/ceramic metamaterial, *Adv. Mater.* **29**, 1605506 (2017)
56. C. Sun, Y. Huang, Q. Shen, W. Wang, W. Pan, P. Zong, L. Yang, Y. Xing, C. Wan, Embedding two-dimensional graphene array in ceramic matrix, *Sci. Adv.* **6**, eabb1338 (2020)
57. C. Cheng, K. Yan, R. Fan, L. Qian, Z. Zhang, K. Sun, M. Chen, Negative permittivity behavior in the carbon/silicon nitride composites prepared by impregnation-carbonization approach, *Carbon* **96**, 678 (2016)
58. C. Cheng, R. Fan, Z. Wang, Q. Shao, X. Guo, P. Xie, Y. Yin, Y. Zhang, L. An, Y. Lei, J.E. Ryu, A. Shankar, Z. Guo, Tunable and weakly negative permittivity in carbon/silicon nitride composites with different carbonizing temperatures, *Carbon* **125**, 103 (2017)
59. C. Cheng, R. Fan, Z. Wang, P. Xie, C. Hou, G. Fan, Y. Lei, L. An, Y. Liu, Radio-frequency negative permittivity in the graphene/silicon nitride composites prepared by spark plasma sintering, *J. Am. Ceram. Soc.* **101**, 1598 (2018)



60. C. Cheng, R. Fan, Y. Ren, T. Ding, L. Qian, J. Guo, X. Li, L. An, Y. Lei, Y. Yin, Z. Guo, Radio frequency negative permittivity in random carbon nanotubes/alumina nanocomposites, *Nanoscale* **9**, 5779 (2017)
61. R. Yin, Y. Zhang, W. Zhao, X. Huang, X. Li, L. Qian, Graphene platelets/aluminium nitride metacomposites with double percolation property of thermal and electrical conductivity, *J. Eur. Ceram. Soc.* **38**, 4701 (2018)
62. Y. Qu, J. Lin, J. Wu, Z. Wang, K. Sun, M. Chen, B. Dong, Z. Guo, R. Fan, Graphene-carbon black/CaCu<sub>3</sub>Ti<sub>4</sub>O<sub>12</sub> ternary metacomposites toward a tunable and weakly  $\epsilon$ -negative property at the radio-frequency region, *J. Phys. Chem. C* **124**, 23361 (2020)
63. R. Singh, A. Chakravarty, S. Mishra, R.C. Prajapati, J. Dutta, I.K. Bhat, U. Pandel, S.K. Biswas, K. Muraleedharan, AlN-SWCNT metacomposites having tunable negative permittivity in radio and microwave frequencies, *ACS Appl. Mater. Interfaces* **11**, 48212 (2019)
64. C. Cheng, R. Fan, L. Qian, X. Wang, L. Dong, Y. Yin, Tunable negative permittivity behavior of random carbon/alumina composites in the radio frequency band, *RSC Adv.* **6**, 87153 (2016)
65. Z. Dang, J. Yuan, J. Zha, T. Zhou, S. Li, G. Hu, Fundamentals, processes and applications of high-permittivity polymer-matrix composites, *Prog. Mater. Sci.* **57**, 660 (2012)
66. P. Wang, Z. Pan, M. Wang, S. Huang, J. Liu, J. Zhai, Polypyrrole random-coil induced permittivity from negative to positive in all-organic composite films, *J. Materiomics* **6**, 348 (2020)
67. F. Liu, Q. Li, J. Cui, Z. Li, G. Yang, Y. Liu, L. Dong, C. Xiong, H. Wang, Q. Wang, High-energy-density dielectric polymer nanocomposites with trilayered architecture, *Adv. Funct. Mater.* **27**, 1606292 (2017)
68. H. Gu, H. Zhang, C. Ma, S.Y. Lyu, F. Yao, C. Liang, X. Yang, J. Guo, Z. Guo, J. Gu, Polyaniline assisted uniform dispersion for magnetic ultrafine barium ferrite nanorods reinforced epoxy metacomposites with tailorable negative permittivity, *J. Phys. Chem. C* **121**, 13265 (2017)
69. K. Sun, P. Xie, Z. Wang, T. Su, Q. Shao, J.E. Ryu, X. Zhang, J. Guo, A. Shankar, J. Li, R. Fan, D. Cao, Z. Guo, Flexible polydimethylsiloxane/multi-walled carbon nanotubes membranous metacomposites with negative permittivity, *Polymer* **125**, 50 (2017)
70. K. Sun, J. Dong, Z. Wang, Z. Wang, G. Fan, Q. Hou, L. An, M. Dong, R. Fan, Z. Guo, Tunable negative permittivity in flexible graphene/PDMS metacomposites, *J. Phys. Chem. C* **123**, 23635 (2019)
71. K. Sun, Z. Wang, J. Xin, Z. Wang, P. Xie, G. Fan, V. Murugadoss, R. Fan, J. Fan, Z. Guo, Hydrosoluble graphene/polyvinyl alcohol membranous composites with negative permittivity behavior, *Macromol. Mater. Eng.* **305**, 1900709 (2020)
72. K. Sun, J. Qin, Z. Wang, Y. An, X. Li, B. Dong, X. Wu, Z. Guo, R. Fan, Polyvinyl alcohol/carbon fibers composites with tunable negative permittivity behavior, *Surf. Interfaces* **21**, 100735 (2020)
73. Z. Wang, K. Sun, H. Wu, P. Xie, Z. Wang, X. Li, R. Fan, Compressible sliver nanowires/polyurethane sponge metacomposites with weakly negative permittivity controlled by elastic deformation, *J. Mater. Sci.* **55**, 15481 (2020)
74. Y. Sun, J. Wang, S. Qi, G. Tian, D. Wu, Permittivity transition from highly positive to negative: polyimide/carbon nanotube composite's dielectric behavior around percolation threshold, *Appl. Phys. Lett.* **107**, 012905 (2015)
75. Z. Jiao, D.R. D'Hooge, L. Cardon, J. Qiu, Elegant design of carbon nanotube foams with double continuous structure for metamaterials in a broad frequency range, *J. Mater. Chem. C* **8**, 3226 (2020)
76. H. Massango, T. Tsutaoka, T. Kasagi, S. Yamamoto, K. Hatakeyama, Complex permeability and permittivity spectra of percolated Fe<sub>50</sub>Co<sub>50</sub>/Cu granular composites, *J. Magn. Magn. Mater.* **442**, 403 (2017)
77. P. Xie, K. Sun, Z. Wang, Y. Liu, R. Fan, Z. Zhang, G. Schumacher, Negative permittivity adjusted by SiO<sub>2</sub>-coated metallic particles in percolative composites, *J. Alloys Compd.* **725**, 1259 (2017)
78. P. Xie, Z. Wang, K. Sun, C. Cheng, Y. Liu, R. Fan, Regulation mechanism of negative permittivity in percolating composites via building blocks, *Appl. Phys. Lett.* **111**, 112903 (2017)
79. H. Wu, R. Yin, Y. Zhang, Z. Wang, P. Xie, L. Qian, Synergistic effects of carbon nanotubes on negative dielectric properties of graphene-phenolic resin composites, *J. Phys. Chem. C* **121**, 12037 (2017)
80. C. Xu, G. Fan, Y. Qu, Y. Liu, Z. Zhang, R. Fan, Core-shell structured tungsten carbide/polypyrrole metacomposites with tailorable negative permittivity at the radio frequency, *Polymer* **188**, 122125 (2020)
81. K. Yan, R. Fan, M. Chen, K. Sun, L. Yin, H. Li, S. Pan, M. Yu, Perovskite (La, Sr)MnO<sub>3</sub> with tunable electrical properties by the Sr-doping effect, *J. Alloys Compd.* **628**, 429 (2015)
82. K. Yan, R. Fan, Z. Shi, M. Chen, L. Qian, Y. Wei, K. Sun, J. Li, Negative permittivity behavior and magnetic performance of perovskite La<sub>1-x</sub>Sr<sub>x</sub>MnO<sub>3</sub> at high-frequency, *J. Mater. Chem. C* **2**, 1028 (2014)
83. Z. Wang, K. Sun, P. Xie, R. Fan, Y. Liu, Q. Gu, J. Wang, Low-loss and temperature-stable negative permittivity in La<sub>0.5</sub>Sr<sub>0.5</sub>MnO<sub>3</sub> ceramics, *J. Eur. Ceram. Soc.* **40**, 1917 (2020)
84. V.V. Varadan, L. Ji, Temperature dependence of resonances in metamaterials, *IEEE Trans. Microwave Theory Tech.* **58**, 2673 (2010)
85. G. Fan, Z. Wang, K. Sun, Y. Liu, R. Fan, Doped ceramics of indium oxides for negative permittivity materials in MHz-kHz frequency regions, *J. Mater. Sci. Technol.* **61**, 125 (2021)
86. G. Fan, Z. Wang, K. Sun, Y. Liu, R. Fan, Doping-dependent negative dielectric permittivity realized in mono-phase antimony tin oxide ceramics, *J. Mater. Chem. C* **8**, 11610 (2020)
87. M. Kılıç, Z.G. Özdemir, Y. Karabul, Ö. Karatas, Ö.A. Çataltepe, Negative real permittivity in (Bi<sub>0.3</sub>Eu<sub>0.7</sub>)Sr<sub>2</sub>CaCu<sub>2</sub>O<sub>6.5</sub> ceramic, *Physica B* **584**, 412080 (2020)
88. R.S. Kohlman, J. Joo, Y.Z. Wang, J.P. Pouget, H. Kaneko, T. Ishiguro, A.J. Epstein, Drude metallic response of polypyrrole, *Phys. Rev. Lett.* **74**, 773 (1995)

89. M. Dressel, M. Dressel, A. Schwartz, A. Schwartz, G. Grüner, G. Grüner, L. Degiorgi, Deviations from drude response in low-dimensional metals: electrodynamics of the metallic state of  $(\text{TMTSF})_2\text{PF}_6$ , *Phys. Rev. Lett.* **77**, 398 (1996)
90. X. Xu, Q. Fu, H. Gu, Y. Guo, H. Zhou, J. Zhang, D. Pan, S. Wu, M. Dong, Z. Guo, Polyaniline crystalline nanostructures dependent negative permittivity metamaterials, *Polymer* **188**, 122129 (2020)
91. C. Cheng, R. Fan, G. Fan, H. Liu, J. Zhang, J. Shen, Q. Ma, R. Wei, Z. Guo, Tunable negative permittivity and magnetic performance of yttrium iron garnet/polypyrrole metacomposites at the RF frequency, *J. Mater. Chem. C* **7**, 3160 (2019)
92. P. Sreekala, J. Honey, C. Aanandan, Development and characterization of camphor sulphonic acid doped polyaniline film with broadband negative dielectric constant for microwave applications, *Mater. Res. Express* **5**, 056302 (2018)
93. K. Lee, J. Heeger, Crossover to negative dielectric response in the low-frequency spectra of metallic polymers, *Phys. Rev. B* **68**, 035201 (2003)
94. K.L. Gordon, J.H. Kang, C. Park, P.T. Lillehei, J.S. Harrison, A novel negative dielectric constant material based on phosphoric acid doped poly(benzimidazole), *J. Appl. Polym. Sci.* **125**, 2977 (2012)
95. Z. Wang, W. Zhou, L. Dong, X. Sui, H. Cai, J. Zuo, Q. Chen, Dielectric spectroscopy characterization of relaxation process in Ni/epoxy composites, *J. Alloys Compd.* **682**, 738 (2016)
96. Y. Wan, W. Yang, S. Yu, R. Sun, C. Wong, W. Liao, Covalent polymer functionalization of graphene for improved dielectric properties and thermal stability of epoxy composites, *Compos. Sci. Technol.* **122**, 27 (2016)
97. Q. Zhang, J. Wang, B. Guo, Z. Guo, J. Yu, Electrical conductivity of carbon nanotube-filled miscible poly(phenylene oxide)/polystyrene blends prepared by melt compounding, *Composites Part B* **176**, 107213 (2019)
98. Z. Wang, K. Sun, P. Xie, Y. Liu, Q. Gu, R. Fan, Permittivity transition from positive to negative in acrylic polyurethane-aluminum composites, *Compos. Sci. Technol.* **188**, 107969 (2020)
99. Z. Wang, P. Xie, C. Cheng, G. Fan, Z. Zhang, R. Fan, X. Yin, Regulation mechanism of negative permittivity in poly(p-phenylene sulfide)/multiwall carbon nanotubes composites, *Synth. Met.* **244**, 15 (2018)
100. Y. Qu, Y. Wu, G. Fan, P. Xie, Y. Liu, Z. Zhang, J. Xin, Q. Jiang, K. Sun, R. Fan, Tunable radio-frequency negative permittivity of Carbon/ $\text{CaCu}_3\text{Ti}_4\text{O}_{12}$  metacomposites, *J. Alloys Compd.* **834**, 155164 (2020)
101. C. Hou, G. Fan, X. Xie, X. Zhang, X. Sun, Y. Zhang, B. Wang, W. Du, R. Fan,  $\text{TiN}/\text{Al}_2\text{O}_3$  binary ceramics for negative permittivity metacomposites at kHz frequencies, *J. Alloys Compd.* **855**, 157499 (2021)
102. H. Luo, J. Qiu, Carbon nanotube/polyolefin elastomer metacomposites with adjustable radio-frequency negative permittivity and negative permeability, *Adv. Electron. Mater.* **5**, 1900011 (2019)
103. Z. Shi, R. Fan, Z. Zhang, H. Gong, J. Ouyang, Y. Bai, X. Zhang, L. Yin, Experimental and theoretical investigation on the high frequency dielectric properties of  $\text{Ag}/\text{Al}_2\text{O}_3$  composites, *Appl. Phys. Lett.* **99**, 137401 (2011)
104. A. Patra, Prasad, Effect of  $\text{LaNiO}_3$  on the impedance and dielectric properties of  $\text{CoFe}_2\text{O}_4$ : a high temperature study, *J. Phys. D: Appl. Phys.* **53**, 45301 (2020)
105. T. Tsutaoka, T. Kasagi, S. Yamamoto, K. Hatakeyama, Double negative electromagnetic property of granular composite materials in the microwave range, *J. Magn. Mater.* **383**, 139 (2015)
106. T. Tsutaoka, H. Massango, T. Kasagi, S. Yamamoto, K. Hatakeyama, Double negative electromagnetic properties of percolated  $\text{Fe}_{53}\text{Ni}_{47}/\text{Cu}$  granular composites, *Appl. Phys. Lett.* **108**, 191904 (2016)
107. Z. Wang, K. Sun, P. Xie, Q. Hou, Y. Liu, Q. Gu, R. Fan, Design and analysis of negative permittivity behaviors in barium titanate/nickel metacomposites, *Acta Mater.* **185**, 412 (2020)
108. B. Zhao, C.B. Park, Tunable electromagnetic shielding properties of conductive poly(vinylidene fluoride)/Ni chain composite films with negative permittivity, *J. Mater. Chem. C* **5**, 6954 (2017)
109. Y. Qing, Q. Wen, F. Luo, W. Zhou, Temperature dependence of the electromagnetic properties of graphene nanosheet reinforced alumina ceramics in the X-band, *J. Mater. Chem. C* **4**, 4853 (2016)
110. C. Cheng, Y. Jiang, X. Sun, J. Shen, T. Wang, G. Fan, R. Fan, Tunable negative permittivity behavior and electromagnetic shielding performance of silver/silicon nitride metacomposites, *Composites Part A* **130**, 105753 (2020)
111. J. Yang, X. Zhu, H. Wang, X. Wang, C. Hao, R. Fan, D. Dastan, Z. Shi, Achieving excellent dielectric performance in polymer composites with ultralow filler loadings via constructing hollow-structured filler frameworks, *Compos. Part A* **131**, 105814 (2020)
112. C. Zhang, Z. Shi, F. Mao, C. Yang, X. Zhu, J. Yang, H. Zuo, R. Fan, Flexible polyimide nanocomposites with dc bias induced excellent dielectric tunability and unique non-percolative negative- $k$  toward intrinsic metamaterials, *ACS Appl. Mater. Interfaces* **10**, 26713 (2018)
113. J. Wang, Z. Shi, F. Mao, S. Chen, X. Wang, Bilayer polymer metacomposites containing negative permittivity layer for new high- $k$  materials, *ACS Appl. Mater. Interfaces* **9**, 1793 (2016)
114. Z. Shi, J. Wang, F. Mao, C. Yang, C. Zhang, R. Fan, Significantly improved dielectric performances of sandwich-structured polymer composites induced by alternating positive- $k$  and negative- $k$  layers, *J. Mater. Chem. A* **5**, 14575 (2017)
115. R. Gong, L. Yuan, G. Liang, A. Gu, Preparation and mechanism of high energy density cyanate ester composites with ultralow loss tangent and higher permittivity through building a multilayered structure with conductive, dielectric, and insulating layers, *J. Phys. Chem. C* **123**, 13482 (2019)
116. P. Xie, Z. Zhang, Z. Wang, K. Sun, R. Fan, Targeted double negative properties in silver/silica random metamaterials by precise control of microstructures, *Research* **2019**, 1021368 (2019)
117. S. Sharma, T. Basu, A. Shahee, K. Singh, N. Lalla, E. Sampathkumaran, Complex dielectric and impedance behavior of magnetoelectric  $\text{Fe}_2\text{TiO}_5$ , *J. Alloys Compd.* **663**, 289 (2016)
118. K. Sun, J. Xin, Y. Li, Z. Wang, Q. Hou, X. Li, X. Wu, R. Fan, K.L. Choy, Negative permittivity derived from inductive



- characteristic in the percolating Cu/EP metacomposites, J. Mater. Sci. Technol. **35**, 2463 (2019)
119. Y. Li, N. Engheta, Capacitor-inspired metamaterial inductors, Phys. Rev. Appl. **10**, 054021 (2018)
120. J. Dai, H. Luo, M. Moloney, J. Qiu, Adjustable graphene/polyolefin elastomer epsilon-near-zero metamaterials at radiofrequency range, ACS Appl. Mater. Interfaces **12**, 22019 (2020)

**Cite this article as:** Guohua Fan, Kai Sun, Qing Hou, Zhongyang Wang, Yao Liu, Runhua Fan, Epsilon-negative media from the viewpoint of materials science, EPJ Appl. Metamat. **8**, 11 (2021)